

AD-A057 662

UNITED TECHNOLOGIES RESEARCH CENTER EAST HARTFORD CONN

F/G 13/13

REDESIGN OF STRUCTURAL VIBRATION MODES BY FINITE ELEMENT INVERS--ETC(U)

MAY 78 K A STETSON, I R HARRISON

F33615-77-C-2092

UNCLASSIFIED

UTRC/R77-992945

AFAPL-TR-78-21

NL

1 of 1

AD
A057 662



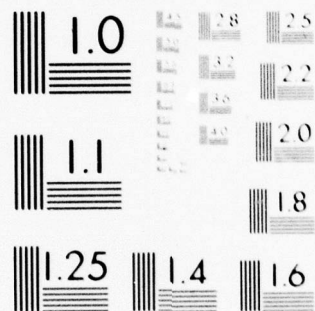
END

DATE

FILMED

9-78

DDC



MICROCOPY RESOLUTION TEST CHART
NATIONAL BUREAU OF STANDARDS-1963-A

AD A057662

AFAPL-TR-78-21

LEVEL II

2

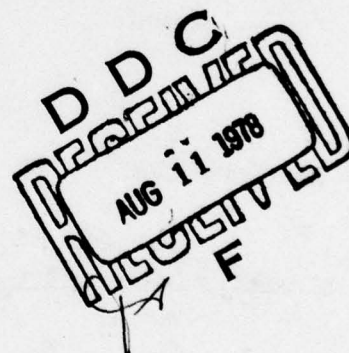
REDESIGN OF STRUCTURAL VIBRATION MODES BY FINITE ELEMENT INVERSE PERTURBATION

K. A. STETSON
I. R. HARRISON
B. N. CASSENTI

UNITED TECHNOLOGIES RESEARCH CENTER
EAST HARTFORD, CONNECTICUT 06108

MAY 1978

TECHNICAL REPORT AFAPL-TR-78-21
Final Report - July 1977 - February 1978



Approved for public release; distribution unlimited.

AIR FORCE AERO PROPULSION LABORATORY
AIR FORCE WRIGHT AERONAUTICAL LABORATORIES
AIR FORCE SYSTEMS COMMAND
WRIGHT-PATTERSON AIR FORCE BASE, OHIO 45433

78 08 08 036

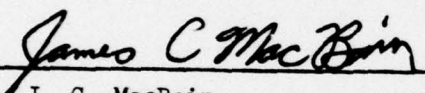
AD No. _____
DDC FILE COPY

NOTICE

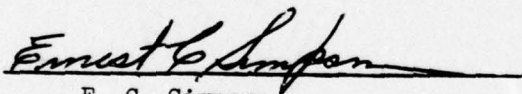
When Government drawings, specifications, or other data are used for any purpose other than in connection with a definitely related Government procurement operation, the United States Government thereby incurs no responsibility nor any obligation whatsoever; and the fact that the government may have formulated, furnished, or in any way supplied the said drawings, specifications, or other data, is not to be regarded by implication or otherwise as in any manner licensing the holder or any other person or corporation, or conveying any rights or permission to manufacture, use, or sell any patented invention that may in any way be related thereto.

This report has been reviewed by the Information Office (OI) and is releasable to the National Technical Information Service (NTIS). At NTIS, it will be available to the general public, including foreign nations.

This technical report has been reviewed and is approved for publication.


J. C. MacBain

FOR THE COMMANDER


E. C. Simpson

"If your address has changed, if you wish to be removed from our mailing list, or if the addressee is no longer employed by your organization please notify AFAPL/TBP, W-PAFB, OH 45433 to help us maintain a current mailing list".

Copies of this report should not be returned unless return is required by security considerations, contractual obligations, or notice on a specific document.

UNCLASSIFIED

SECURITY CLASSIFICATION OF THIS PAGE (When Data Entered)

REPORT DOCUMENTATION PAGE		READ INSTRUCTIONS BEFORE COMPLETING FORM	
1. REPORT NUMBER	2. GOVT ACCESSION NO.	3. RECIPIENT'S CATALOG NUMBER	
AFAPL TR-78-21			
4. TITLE (and Subtitle)		5. TYPE OF REPORT & PERIOD COVERED	
REDESIGN OF STRUCTURAL VIBRATION MODES BY FINITE ELEMENT INVERSE PERTURBATION.		Final Technical Report. 12 July 1977-12 Feb 1978	
6. AUTHOR(s)		7. PERFORMING ORG. REPORT NUMBER	
K. A. Stetson, I. R. Harrison, B. N. Cassenti		RT7-992945	
8. CONTRACT OR GRANT NUMBER(s)		9. PROGRAM ELEMENT, PROJECT, TASK AREA & WORK UNIT NUMBERS	
F33615-77-C-2092		2307 S2-05	
10. PERFORMING ORGANIZATION NAME AND ADDRESS		11. CONTROLLING OFFICE NAME AND ADDRESS	
United Technologies Research Center, a Division of United Technologies Corporation East Hartford, Connecticut 06108		Air Force Aero Propulsion Laboratory (TBP) Wright-Patterson AFB, Ohio 45433	
12. MONITORING AGENCY NAME & ADDRESS (if different from Controlling Office)		13. REPORT DATE	
1274p.		MAY 1978	
14. DISTRIBUTION STATEMENT (of this Report)		15. SECURITY CLASS. (of this report)	
Approved for public release; distribution unlimited.		Unclassified	
16. DISTRIBUTION STATEMENT (of the abstract entered in Block 20, if different from Report)		17. SUPPLEMENTARY NOTES	
18. KEY WORDS (Continue on reverse side if necessary and identify by block number)		19. DECLASSIFICATION/DOWNGRADING SCHEDULE	
Inverse Perturbation Design Finite Element Analysis Structural Design		Vibration Analysis Holography Curved Shell Design	
20. ABSTRACT (Continue on reverse side if necessary and identify by block number)			
It has been demonstrated that it is feasible to apply the inverse perturbation method, originally developed at United Technologies Research Center, directly to the output of a finite element computer analysis of a structure. Thus, a new structural design tool has been developed which has the potential for application to the mathematically complex structure of a turbine blade. The initial step in this direction, as described herein, was the redesign of a flat plate and a 45° arc of a cylindrical shell, both mounted as cantilever beams. Included in the report, in addition to a detailed (over) → over			

DD FORM 1 JAN 73 1473

EDITION OF 1 NOV 65 IS OBSOLETE

UNCLASSIFIED

SECURITY CLASSIFICATION OF THIS PAGE (When Data Entered)

409 252

LB

UNCLASSIFIED

SECURITY CLASSIFICATION OF THIS PAGE(When Data Entered)

review of the contract work, is an overview of the concept of inverse perturbation, and a detailed description of previous UTRC work on redesigning structural vibration modes by inverse perturbation subject to minimal change theory, which set the stage for the present investigations. The work was performed under Contract F33615-77-C-2092 for the Air Force Aero Propulsion Laboratory at Wright-Patterson Air Force Base.

UNCLASSIFIED

SECURITY CLASSIFICATION OF THIS PAGE(When Data Entered)

PREFACE

This final report was submitted by United Technologies Research Center, United Technologies Corporation, E. Hartford, Connecticut under Contract Number F33615-77-C-2092. The effort was sponsored by the Air Force Aero Propulsion Laboratory, Air Force Systems Command, Wright-Patterson AFB, Ohio, under Project 2307, Task S2, and Work Unit 05 with Dr. James C. MacBain/AFAPL/TBP as project engineer in charge. Dr. K. A. Stetson, Ms. I. R. Harrison, Mr. B. N. Cassenti, and Mr. R. K. Erf of United Technologies Research Center were technically responsible for the work.

ACCESSION for	
NTIS	White Section <input checked="" type="checkbox"/>
DDC	Buff Section <input type="checkbox"/>
UNANNOUNCED	
JUSTIFICATION	
BY	
DISTRIBUTION/AVAILABILITY CODES	
SPECIAL	
A	

TABLE OF CONTENTS

SECTION		PAGE
I	SUMMARY	1
II	INTRODUCTION	2
III	THE CONCEPT OF INVERSE PERTURBATION	4
IV	COMPUTER PROGRAM DESCRIPTIONS	8
	POSTPR Program	8
	NASTY Program	8
	CHANGNAST Program	8
	TESTNASTY Program	9
	C2 Program	9
	DISP2V Program	9
V	ANALYTICAL-EXPERIMENTAL INVESTIGATIONS	10
	NASTRAN Modeling of the Vibration Modes	10
	Holographic Analysis and NASTRAN Comparison	14
	System Checks	19
	Structural Redesign and Correlation	21
VI	CONCLUSIONS AND RECOMMENDATIONS	25
APPENDIX	REDESIGNING STRUCTURAL VIBRATION MODES BY INVERSE PERTURBATION, SUBJECT TO MINIMAL CHANGE THEORY	27
	Abstract	27
	Introduction	27
	Theory	28
	Experimental Application	33
	Theory of Minimal Adjustments	56
	Conclusions	60
	References	61

PRECEDING PAGE BLANK

LIST OF ILLUSTRATIONS

<u>Figure</u>		<u>Page</u>
1	Plate and Shell as Divided into Elements	11
2a	Experimental Cantilever Plate	12
2b	Experimental Cantilever Shell Segment	13
3	Holographic Reconstructions of Plate Modes	15
4a	Holographic Reconstructions of 1st Shell Mode	16
4b	Holographic Reconstructions of 2nd Shell Mode	17
4c	Holographic Reconstructions of 3rd Shell Mode	18
5a	Fractional Thickness Change for New Plate Design	22
5b	Fractional Thickness Change for New Shell Design	23
1A	Contour Plots of Modes 1 & 2 for a Square Plate	36
2A	Holographic Reconstruction of Circular Disk, 1st 2D Mode . .	38
3Aa	Perturbation Function for Square Plate, 1st Mode Frequency .	39
3Ab	Perturbation Function for Square Plate, 2nd Mode Frequency .	40
3Ac	Perturbation Function for Square Plate, 2nd Mode to 1st Mode	41
3Ad	Perturbation Function for Square Plate, 1st Mode to 2nd Mode	42
4Aa	Analytic vs. Computer Values, 1st Mode Frequency	44
4Ab	Analytic vs. Computer Values, 2nd Mode Frequency	45
4Ac	Analytic vs. Computer Values, 2nd Mode to 1st Mode	46
4Ad	Analytic vs. Computer Values, 1st Mode to 2nd Mode	47
5A	New Node Line Plot for Modified Cantilever Plate	49
6A	Modified Cantilever Plate	51
7A	Holographic Reconstruction of Cantilever Plate, 2nd Mode . .	52

LIST OF TABLES

<u>Table</u>		<u>Page</u>
I	Structural Mode Frequencies	10
II	NASTRAN-Holographic Differences for Plate Modes	19
III	NASTRAN-Holographic Differences for Shell Modes	20
IV	Orthogonality and Rayleigh Quotient Checks	21
V	Results of Design Changes	24
IA	Random Error Effect on the MODES Program	35
IIA	Analytic vs. Computer Values of Perturbations	43
IIIA	Fractional Thickness Changes, Contoured Plate	50
IVA	Experimental Perturbations vs. 3 1st Order Calculations	53
VA	Orthogonality and Rayleigh-Quotient Checks	55
VIA	CHECK Program Results After 2nd Partial Adjustments	58
VIIA	Perturbations Calculated with Adjusted 2nd Partial Derivatives	58

LIST OF SYMBOLS

x,y,z	coordinates of a plate or shell
$h(x,y)$	thickness of a plate or shell
$\Delta h(x,y)$	change in thickness
$\phi(x,y)$	perturbation function
(Δ)	row matrix of changes in mode shape and frequency
$[B]$	perturbation matrix
$\Phi(x,y)$	vibration mode shape
Δ	element of row matrix of changes
b	element of perturbation matrix
$\hat{i}, \hat{j}, \hat{k}$	unit vectors in x, y, and z directions
a,b,c	coefficients of polynomials of element deformations
ω	modal frequency in radians per second
ρ	volume density
M	modal mass
G	matrix of stiffness moduli
E	Young's modulus
ν	Poisson's ratio
C	Admixture coefficient

Subscript

n,k	nth or kth mode
nk,lm	mode pair nk or lm
p,q	mode pair p (=nk) or q (=lm)
pq	element of perturbation matrix denoting pth column and qth row

LIST OF SYMBOLS (Cont'd)

n_x, n_y, n_z components of vectorial mode shape in x, y, and z directions
 n_1, \dots, n_9 order of coefficients in polynomial expansions of element deformations
 m, s_b, s_m inertial, bending strain, and membrane strain components of perturbation function
 s, b denoting in-plane strain and bending strain moduli

Superscript

-1 matrix inverse
T matrix transpose
(") second derivative
 xx, yy, xy second partial derivatives with respect to superscript variables
(') first derivative
 x, y partial derivative with respect to superscript variable
' new mode shape

SECTION I

SUMMARY

Presented herein are the results of a four-month technical program to develop and demonstrate the application of an inverse perturbation design procedure, originally developed at United Technologies Research Center, to curved structures. Briefly, the inverse perturbation technique relies on information concerning the existing vibration modes of a structure to calculate the necessary changes to obtain new, prescribed vibration characteristics for selected modes of the structure, and its application to curved structures necessitates the use of finite-element computer analyses to obtain the necessary accuracy. Consequently, the study involved formulation of the equations and computer programs necessary to process NASTRAN output data on vibration mode shapes, and preparation of the UTRC inverse perturbation design program to accept the processed output, and compute: a) the perturbation functions associated with changes in frequency and mode shape admixture (admixture between mode shapes implies that the mode shapes of an altered structure may be expressed as linear combinations of the mode shapes of an unaltered structure), and b) the perturbations that result from design changes, as well as perform checks on the stiffness orthogonality and Rayleigh quotient.

Supported under Contract F33615-77-C-2092, sponsored by the Air Force Aero Propulsion Laboratory, Air Force Systems Command, the program successfully demonstrated concept feasibility with the redesign of a flat plate and a 45° arc of a cylindrical shell, both mounted as cantilever beams. Presented in the following sections are: an introduction which briefly reviews the motivation for the investigations (Section II); an overview of the concept of inverse perturbation (Section III); a description of the computer programs written to implement the concept (Section IV); a presentation of the computations and experiments performed, together with the results obtained for the two cantilevered objects (Section V); and a discussion of potential benefits to be derived from continued development of the technique (Section VI). Included as an Appendix is a detailed description of previous UTRC work on redesigning structural vibration modes by inverse perturbation, subject to minimal change theory, which set the stage for the investigations reported herein.

SECTION II

INTRODUCTION

The design of structures to withstand the vibratory excitation experienced inside a jet engine is clearly a multifaceted problem. Not only must resonant response be considered, but also the possibility of aerodynamically excited vibrations such as flutter. Furthermore, performance requirements, such as the ability of a fan to compress air or of a turbine to extract energy from an air flow, and practical issues, such as weight and resistance to impact damage, also enter into the choice of a good design. The scope of the problem makes a truly general-purpose computerized design procedure unlikely; however, situations do arise where answers to a portion of the total problem can be useful in formulating the proper design approach.

Among the most enigmatic facets of a structure are its vibration modes. These are functions of the structure that can be used to characterize its response to forced vibratory excitation (Ref. 1), to transients, and even to static forces (Ref. 2). So central are these functions in characterizing vibratory response, that in recent years numerous large-scale computer programs have been developed to analyze structures, by finite-element methods, to determine these modes. From the experimental point of view, holographic vibration analysis has greatly facilitated the determination of vibration modes on the visible surfaces of structures (Ref. 1).

Whereas finite-element and holographic methods, in addition to numerous other experimental and theoretical techniques, make it possible to analyze a given structure for its vibration modes, the question of how that structure should be changed to effect a specified change in its vibration modes lies relatively unapproached. Work at the United Technologies Research Center in recent years (Refs. 3, 4 and 5) has suggested a potentially powerful tool, based upon perturbation equations, for just such a task. It is possible, of course, to use perturbation theory to gain an approximate answer to the question of how the vibration modes of a structure will change as a result of small changes in the structure; this has been known since the 19th century. The interesting problem is, however: how does one invert the usual perturbation analysis to answer the question posed at the beginning of this paragraph? The most recent work in this area, at these laboratories, has established that by minimizing the change to a structure necessary to accomplish a set of changes to its vibration modes, we may define a unique set of functions which in turn generate a unique change to the structure. These functions may be called perturbation functions, and they are formed from pairs of vibration-mode functions and their spatial derivatives. A detailed description of that design technique, which we call inverse perturbation, together with its application to the redesign of a cantilever plate, based upon vibration mode data obtained from hologram interferometry is included as Appendix I to the present report.

Presented in the main body of the current report is a description of the program of research carried out under Air Force Contract F33615-77-C-0292 to extend this inverse perturbation method of design, developed for holographically determined vibration modes, so that it can make use of the NASTRAN finite-element program for vibration analysis. This has resulted in a design program which, in its present form, can be used in conjunction with NASTRAN to alter the thickness of any shell-like structure in a way that will generate, approximately, some specified change in the vibration modes of a structure. At present, changes in lateral dimensions of the shell, or in the boundary conditions of the shell cannot be dealt with, but future programs can be conceived to make this possible. The current program is likely to require a number of iterative designs, each involving a NASTRAN analysis to finally close upon a structure whose actual vibrations are the ones desired; however, all indications are that the procedure will converge.

SECTION III

THE CONCEPT OF INVERSE PERTURBATION

The details of the derivations involved in inverse perturbation can be found in Refs. 4 and 5, as well as Appendix I to the present report. Presented here are the general results and the specific equations that relate to this program. First, the design variable is taken to be the percentage change in thickness of the plate or shell, $\Delta h(x,y)/h(x,y)$, where $h(x,y)$ is the thickness of the structure, and x and y are spatial coordinates in its surface. This design variable is expanded as a series of functions, $\theta(x,y)$, called perturbation functions, which are functions of the coordinates, x and y . The coefficients of the series are determined, in part, by the set of changes that are desired, (Δ) , which can be written as a row matrix. The (Δ) 's are related to percentage changes in frequency, and to coefficients of admixture between mode shapes. (As noted in the Summary, admixture between mode shapes implies that the mode shapes of an altered structure may be expressed as linear combinations of the mode shapes of an unaltered structure.) The final set of factors in the equation that determines the percentage changes in thickness is the inverse of what we may call a perturbation matrix, $[B]$. Thus the primary equation of inverse perturbation is

$$\Delta h(x,y)/h(x,y) = (\Delta)[B]^{-1}(\theta(x,y))^T. \quad (1)$$

In Eq. (1), the necessary set of perturbation functions have been arranged as a row matrix, $(\theta(x,y))$, and the superscript T denotes the transposed matrix; i.e., a column matrix. In order to define the matrix $[B]$, it is necessary to specify the set of changes (Δ) and the set of perturbation functions (θ) . (Note: the functional dependence of θ on x and y is implied throughout.) The perturbation functions are formed from products of parameters obtained from pairs of vibration modes, or from squares and products of parameters obtained from a single mode. Thus, we may identify perturbation functions by a double subscript θ_{nk} , or θ_{nn} , depending upon whether the perturbation function is formed from two vibration mode shapes $\phi_n(x,y)$ and $\phi_k(x,y)$, or from $\phi_n(x,y)$ alone. Similarly, the change parameters (Δ) may be characterized by double subscripts; Δ_{nk} being related to the amount of mode shape ϕ_k that is found added to ϕ_n as a result of the structural change, and Δ_{nn} being related to the change in frequency of the n th mode. The specification of any change parameter requires the inclusion of the corresponding perturbation function in Eq. (1). In this way, the number of degrees of freedom in changing the structure (i.e., the perturbation functions) matches the number of constraints (i.e., the change parameters).

With this in mind, let us define the elements of the perturbation matrix, b_{pq} . The double subscripts of the change variables, and the perturbation functions, may be ordered in some arbitrary, but mutually consistent way. Let the double subscript 'nk' correspond to the single index 'p', and some other subscript pair 'lm' correspond to 'q'. Then, the element b_{pq} is defined by

$$b_{pq} = \iint \theta_p(x,y) \theta_q(x,y) dx dy, \quad (2)$$

where the integration is carried out over the surface of the structure. In this particular program, however, the structure has been divided into discrete elements so that the integrations will extend only over the elements, and the contributions of the elements summed to obtain the coefficient b_{pq} .

In order to define the perturbation functions, we must first define the mode functions according to the form they take in the NASTRAN program. Each element of the shell-like structures considered in this program is a triangular platelet of uniform thickness which may bend out of its plane to any shape describable by a cubic polynomial (minus the x^2y term), and may deform and rotate homogeneously within its plane. In terms of a coordinate system local to each element, we may define the mode function, vectorially, as

$$\underline{\phi}_n = \hat{i} \phi_{nx} + \hat{j} \phi_{ny} + \hat{k} \phi_{nz}, \quad (3)$$

where \hat{i} , \hat{j} and \hat{k} are unit vectors in the x, y and z directions, with z being out of the plane of the element, and the origin located at one of the corners of the element. The components of $\underline{\phi}_n$ are, in their polynomial forms:

$$\phi_{nx} = a_{n1} + a_{n2}x + a_{n3}y, \quad (4)$$

$$\phi_{ny} = b_{n1} + b_{n2}x + b_{n3}y, \text{ and} \quad (5)$$

$$\begin{aligned} \phi_{nz} = c_{n1} + c_{n2}x + c_{n3}y + c_{n4}x^2 + c_{n5}xy + c_{n6}y^2 + \\ c_{n7}x^3 + c_{n8}xy^2 + c_{n9}y^3. \end{aligned} \quad (6)$$

The perturbation functions, which may now be defined, are most easily expressed as the sum of three terms: 1) an inertial term, θ_m ; 2) a term related to bending strain, θ_{sb} ; and 3) a term related to membrane strain, θ_{sm} . Thus,

$$\theta_p = \theta_{mp} + \theta_{sbp} + \theta_{smp}, \quad (7)$$

where the subscript 'p' denotes the mode pair 'nk'. The perturbation function, it should be noted, is a scalar. The first term of Eq (7) is

$$\theta_{mp} = -(\omega_n \rho h / \omega_k M_k) \underline{\Phi_n} \cdot \underline{\Phi_k}, \quad (8)$$

where ω_n and ω_k are the natural frequencies, in radians, of modes n and k, ρ is volume density, and M_k is the modal mass of the kth mode, defined by

$$M_k = \iint \rho h \underline{\Phi_k} \cdot \underline{\Phi_k} dx dy. \quad (9)$$

To define the second two terms, let us first define the matrix $G_{\lambda s}$ as

$$G_{\lambda s} = [Eh / \omega_n \omega_k M_k (1 - \nu^2)] \begin{bmatrix} 1 & \nu & 0 \\ \nu & 1 & 0 \\ 0 & 0 & (1 - \nu)/2 \end{bmatrix}, \quad (10)$$

where E is Young's modulus and ν is Poisson's ratio. We may now define $G_{\lambda b}$ as

$$G_{\lambda b} = G_{\lambda s} h^2 / 4. \quad (11)$$

Now,

$$\theta_{sbp} = (\Phi_{nz}'') G_{\lambda b} (\Phi_{kz}'')^T, \quad (12)$$

where,

$$\begin{aligned} (\Phi_{kz}'') &= (\Phi_{kz}^{xx}, \Phi_{kz}^{yy}, \Phi_{kz}^{xy}), \text{ and} \\ (\Phi_{nz}'') &= (\Phi_{nz}^{xx}, \Phi_{nz}^{yy}, 2\Phi_{nz}^{xy}), \end{aligned} \quad (13)$$

with the superscripts denoting partial differentiation with respect to the superscript variables. Finally,

$$\theta_{smp} = (\Phi_{nxy}') G_{\lambda s} (\Phi_{kxy}')^T, \quad (14)$$

where,

$$\begin{aligned} (\Phi_{nxy}') &= (\Phi_{nx}^x, \Phi_{ny}^y, \Phi_{ny}^x + \Phi_{nx}^y), \text{ and} \\ (\Phi_{kxy}') &= (\Phi_{kx}^x, \Phi_{ky}^y, \Phi_{ky}^x + \Phi_{kx}^y). \end{aligned} \quad (15)$$

Now let us define the change parameters, (Δ) , in terms of the percentage changes in frequency and coefficients of admixture:

$$\Delta_{nn} = [(1 + \Delta\omega_n/\omega_n)^2 - 1] \quad , \text{ and} \quad (16)$$

$$\Delta_{nk} = C_{nk}(\omega_n^2 - \omega_k^2)/\omega_n\omega_k, \quad (17)$$

where C_{nk} is the admixture coefficient. The new mode shape, $\underline{\phi}_n'$, is expressible in terms of the old mode shapes by the series

$$\underline{\phi}_n' = \underline{\phi}_n + \sum C_{nk} \underline{\phi}_k, \quad (18)$$

where the term for $n = k$ is omitted from the summation.

The format of the NASTRAN analysis requires some degree of approximation in implementing Eq. (1). First of all, whatever new design is generated it should have plate elements of constant thickness, or else the analysis of the new structure becomes very difficult. This means that the values of the perturbation functions in Eq. (1) should be made constant for each element by taking the average value over the element. Another difficulty arises in the computation of the matrix coefficients, b_{pq} , via Eq. (2). If the integrations over each element are carried out as indicated, with products of the polynomials of Eqs. (4-6), then the resulting integrands may be as high as twelfth order polynomials. To avoid the awkwardness of having to deal with such large polynomials, we decided to approximate the perturbation functions within the elements by their average values therein. This made evaluation of the matrix coefficients, via Eq. (2), simpler, and simultaneously provided constant changes in thickness for the plate elements.

SECTION IV

COMPUTER PROGRAM DESCRIPTIONS

A number of computer programs were required in order to implement the design concept of the subject contract. As described in the following paragraphs, they included the primary routines for: 1) accepting the NASTRAN data, processing it and forming coefficient data files (POSTPR); 2) accepting the data files and computing the associated perturbation functions (NASTY); and 3) accepting the perturbation functions and performing the redesign (CHANGNAST), as well as various ancillary routines for performing checks (TESTNASTY, C2 and DISP2V), and subroutines for simplifying some of the programming.

POSTPR Program

This program accepts, as input, the displacements and rotations of the grid points of the finite elements in a NASTRAN vibration-mode analysis, in what is referred to as the global coordinate system. These displacements and rotations are converted to sets of coordinates that are local to each element. The displacements and rotations are then used, together with Eqs. (4-6), to solve for the coefficients that determine the internal deformations of the elements; i.e., the a's, b's, and c's of Eqs. (4-6). This is done for each NASTRAN vibration mode, and the resulting arrays of coefficients are stored in data files for use in subsequent programs.

NASTY Program

This program forms perturbation functions from Eqs. (7-15), and takes their average value over each triangle. Two subroutines (POLVOL and TRIANG) were written to facilitate this computation. POLVOL finds the value of the integral of the product of two polynomials over a triangular region in the x, y plane, while TRIANG, a subroutine to POLVOL, integrates any term of the two-dimensional polynomial over the triangular region. NASTY itself is a subroutine to the main inverse perturbation program (CHANGNAST).

CHANGNAST Program

This is the primary inverse perturbation design program, and it has been written so that it may use perturbation functions generated either by NASTY (and therefore NASTRAN) or by PERTNAST; an updated version of the original program that generates perturbation functions from experimental holographic data. CHANGNAST

accepts the various material parameters (Young's modulus, Poisson's ratio, density, and the vibration mode frequencies), as well as the desired change parameters, i.e., the Δ_{nk} values. It thereupon computes the necessary perturbation functions, forms the perturbation matrix, and generates the new design via Eq. (1), which it can make available on punched cards. It also prints the modal masses, the perturbation matrix, the determinant of the perturbation matrix, the coefficients of the series of the perturbation functions that comprise the new design, and the root-mean-square change in the element thicknesses. Finally, via a subroutine called NASTDL, it computes the various perturbations that may be expected, even for the parameters that are unconstrained, by a formula that is more accurate than the perturbation formula used for the inversion process (see Appendix).

TESTNASTY Program

This program will print the values of the perturbation functions formed by NASTY, and compute the Rayleigh quotients (the ratio of maximum potential energy to maximum kinetic energy in the vibration cycle) and the check for orthogonality of the stiffness functions (see Appendix). It will also compare NASTRAN computations of the vibration modes with holographic data when the vibration mode is a scalar function. It does this by computing the mode-function value of the NASTRAN solution at the center of each section of the structure for which the holographic data has been digitized.

C2 Program

This program takes NASTRAN solutions for the vibration modes of an original and modified structure, and computes the admixture coefficients that best describe the new modes as a series of the old modes.

DISP2V Program

This program computes vectorial displacements, in one plane, of a plate or shell from data provided by two holographic interferograms of a vibration mode. (The third component is assumed to be zero.) By selecting the centers of the sections of the interferograms to be digitized so that they correspond to the NASTRAN grid points, direct comparison can be made to the NASTRAN analysis.

SECTION V

ANALYTICAL-EXPERIMENTAL INVESTIGATIONS

NASTRAN Modeling of the Vibration Modes

The first computations performed were the NASTRAN analyses of both a uniform plate and a uniform shell segment. The plate was 15.24 cm long by 12.7 cm wide by 0.317 cm thick, and the shell segment was a 45° arc of a cylindrical shell, 7.62 cm long, with an outer radius of 7.62 cm and a thickness of 0.317 cm. Schematic illustrations of the structures, as divided into triangular elements for the NASTRAN analyses, are presented in Fig. 1. Material parameters were taken to be: Young's modulus, E , 6.1×10^{11} dynes/cm²; density, ρ , 2.7 grams/cm³; and Poisson's ratio, ν , 0.31. (These were experimentally determined for an aluminum alloy available in the UTRC shop.) The boundary conditions for the clamped edges were imposed by requiring that the displacements and rotations of the grid points along the clamped edges be zero.

Photographs of the experimental structures, as fabricated to correspond to those analyzed by NASTRAN, are presented in Fig. 2. In fact, the thickness of the experimental plate was 0.330 cm on the average.

The comparison of the mode frequencies of the structures, as obtained via NASTRAN and experimentally, are presented in Table I for the first three vibration modes.

TABLE I

STRUCTURAL MODE FREQUENCIES

Vibration Mode	Plate		Shell	
	NASTRAN	Experimental	NASTRAN	Experimental
f_1	105.6 Hz	120.6 Hz	898.7 Hz	806.0 Hz
f_2	293.3 Hz	333.8 Hz	1280.0 Hz	1380.0 Hz
f_3	642.2 Hz	730.6 Hz	4118.0 Hz	4080.0 Hz

The NASTRAN computations of the frequencies for the vibration modes of the plate are all lower than the experimental values by approximately 14 percent. Four percent of the difference is due to the larger thickness of the experimental plate, while the remaining ten percent is quite probably due to a premature cutoff of the iterative solution for the eigenvector in the NASTRAN computations. The consistency in the error suggests a repetitive problem, and this is supported by the Rayleigh quotient checks presented later.

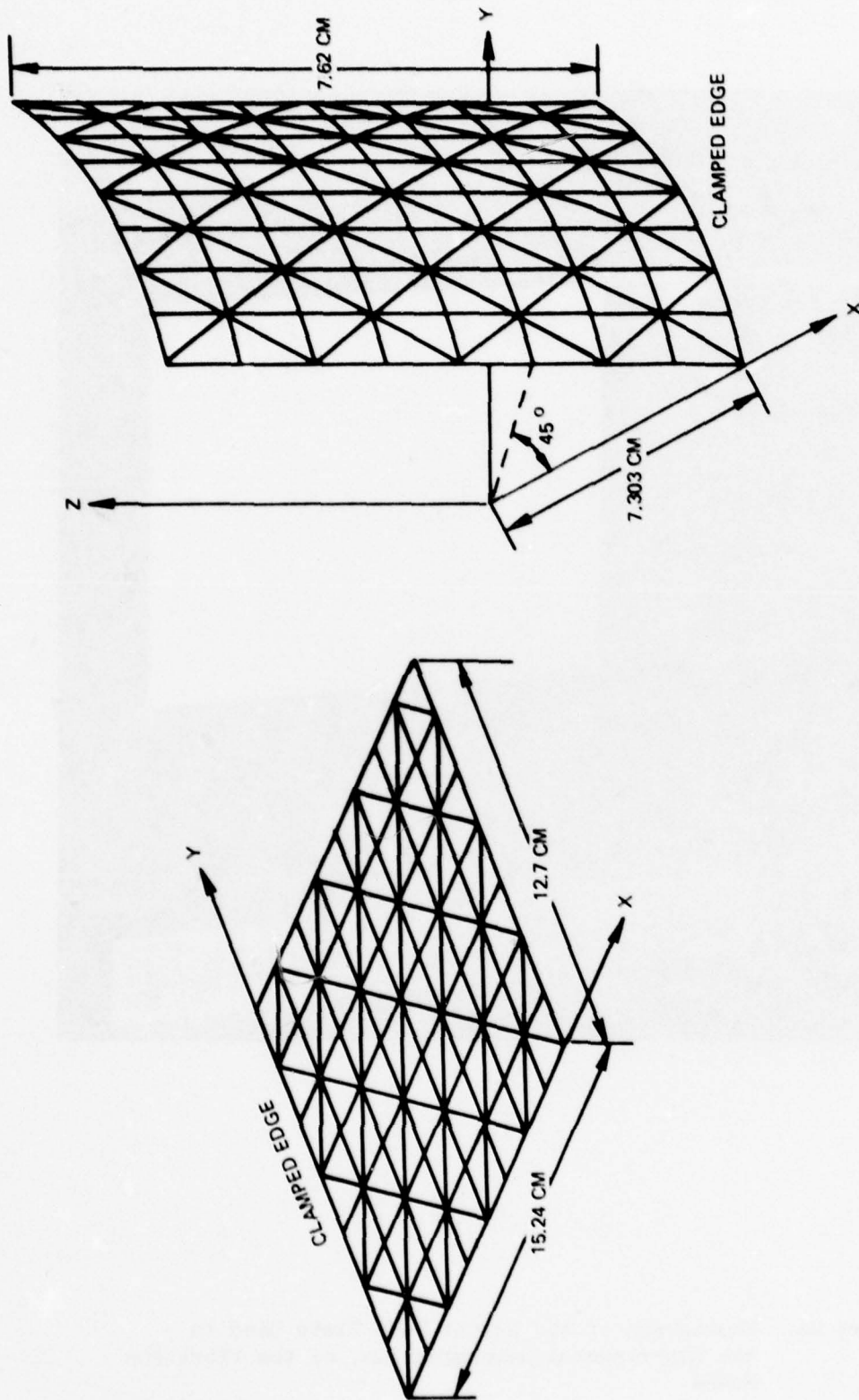


Fig. 1. Division of the Plate and Shell Into the Elements used in the NASTRAN Evaluation of the Vibration Modes

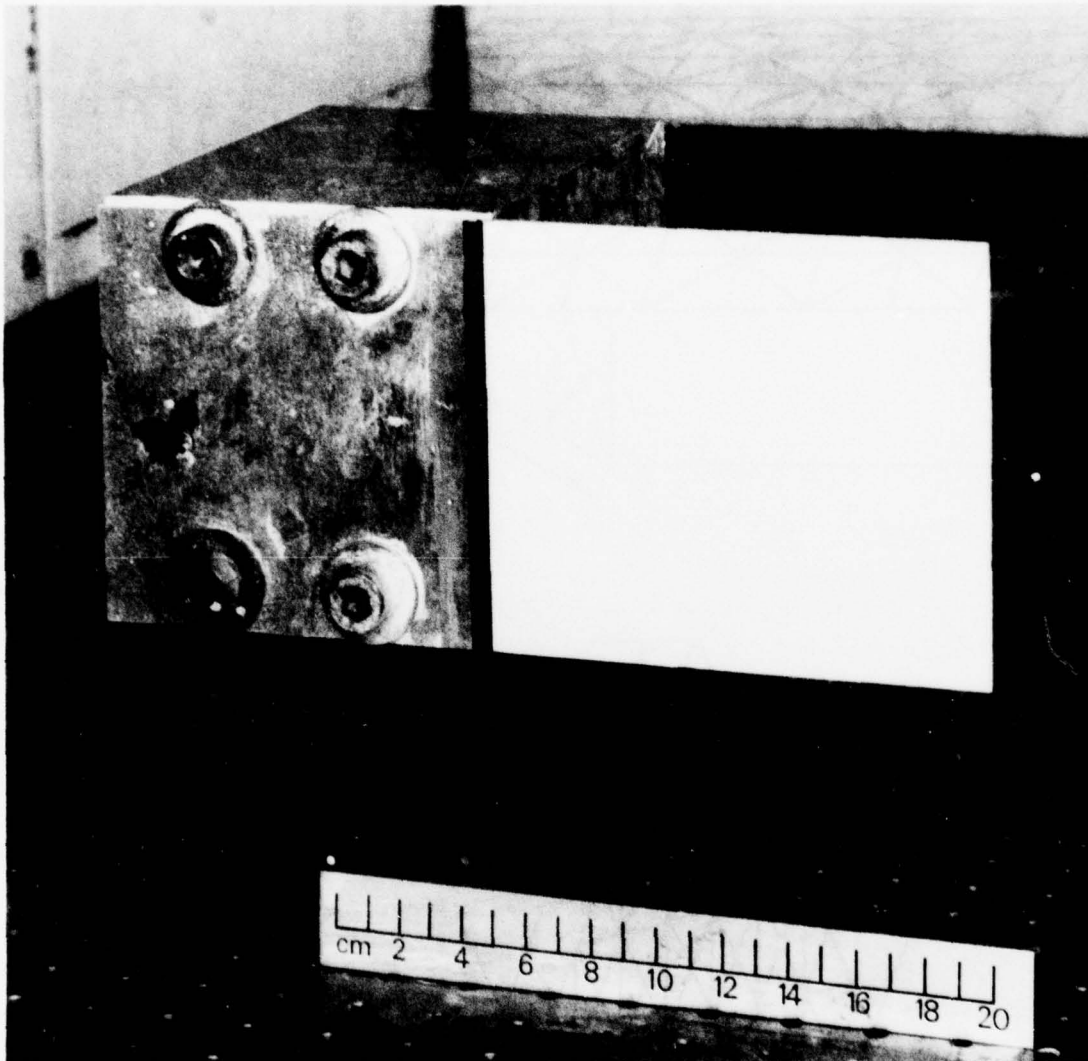


Figure 2a. Photograph of the Actual Test Plate Used in
the Experimental Determination of the Vibration
Modes

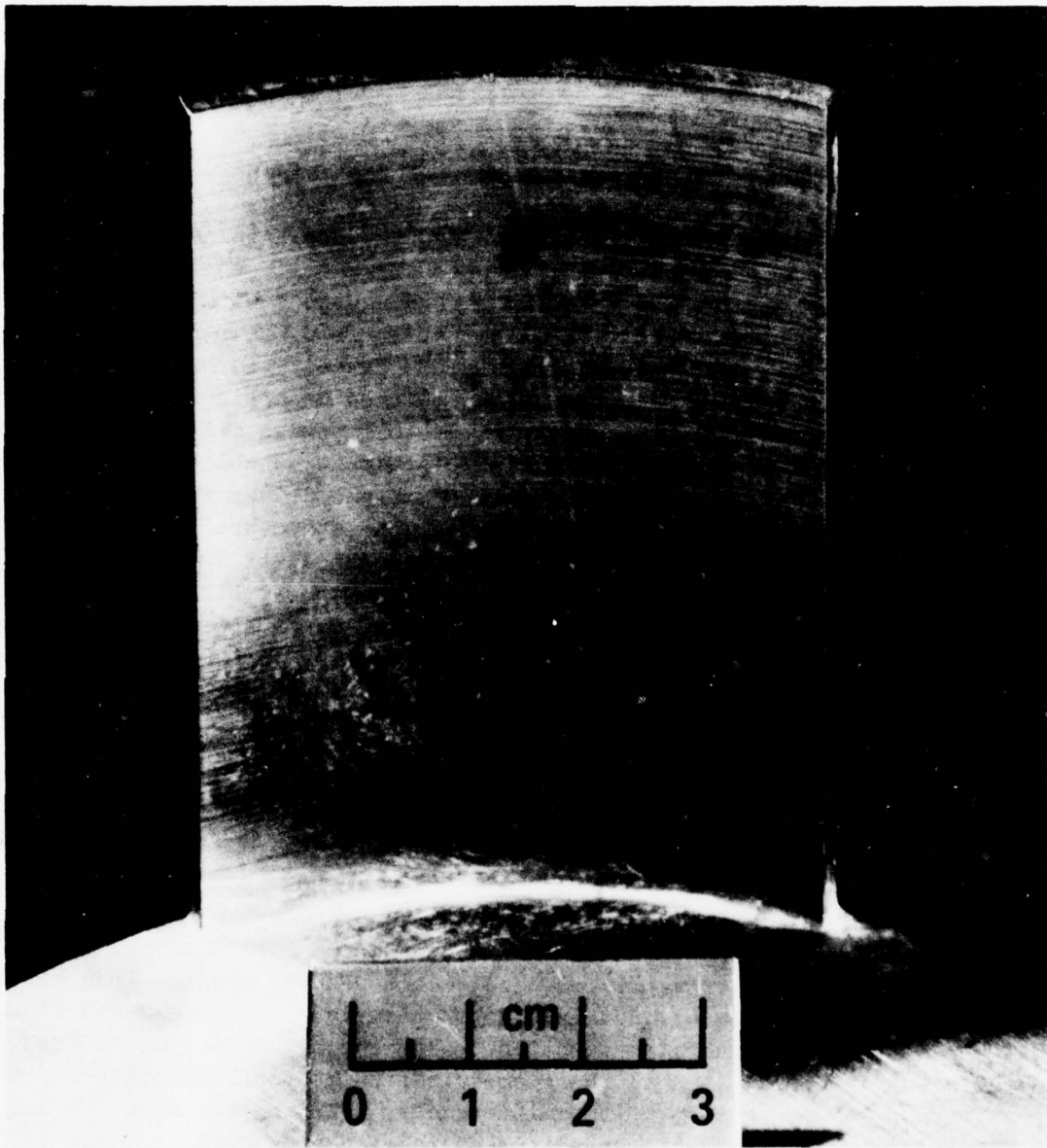


Figure 2b. Photograph of the Actual Test Shell Used in the
Experimental Determination of the Vibration Modes

The NASTRAN computations for the modal frequencies of the shell give results that lie both above and below the experimental values. It is suspected that the first mode frequency, which is in error by over 10 percent, may be the victim of a difficulty in adequately modeling the boundary condition where the shell is attached to the base.

Holographic Analysis and NASTRAN Comparison

Holograms were recorded of both the plate and the shell while each was vibrating in each of its first three modes. In the case of the shell, where both transverse and axial motions are possible, two hologram recordings, one with illumination from the left of the shell and the other with illumination from the right, were made at each resonance. The vibratory state was maintained exactly the same for each recording by means of a feedback circuit which employed an optical vibration probe to detect the vibratory motion, a bandpass filter to suppress all signals except those in the region of a resonance, a limiting circuit to establish a vibratory level, and the conventional amplifiers and electromagnet driver to stimulate the vibration. When the system was properly adjusted, the structure's own vibration mode would determine the frequency of resonance, and the limiting circuit would determine the amplitude. Such a system is inherently more stable than an open loop excitation of the resonance where a small drift of the oscillator frequency can produce a significant change in vibration amplitude. It is important to maintain the same vibration level on the structure for each of the two holograms (with different illuminations) because in their reconstructions the difference in fringe patterns between them is used to determine the motion transverse to the direction of observation.

Plate Holographic Results

Reconstructions from holograms of the plate, recorded while it was vibrating in each of its first three resonance modes, are presented in Fig. 3. They are, respectively, the first bending, first torsion, and second bending modes. From previous work, these patterns had been divided into 36 sections (a 6 x 6 array) and the data digitized and fitted to biquadratic functions. For comparison to the NASTRAN solutions, the latter were evaluated at the geometrical points corresponding to the centers of the digitized sections. The differences, defining the mode fit between the NASTRAN and the normalized holographic results, are presented in Table II. Disagreement between the two can be seen to be less than a few percent of the maximum value (unity) in all cases.

Shell Holographic Results

Reconstructions from the holograms recorded of the shell while it was vibrating in each of its first three modes are presented in Fig. 4. These correspond, morphologically, to the same three modes of the uniform plate. The photographs of these

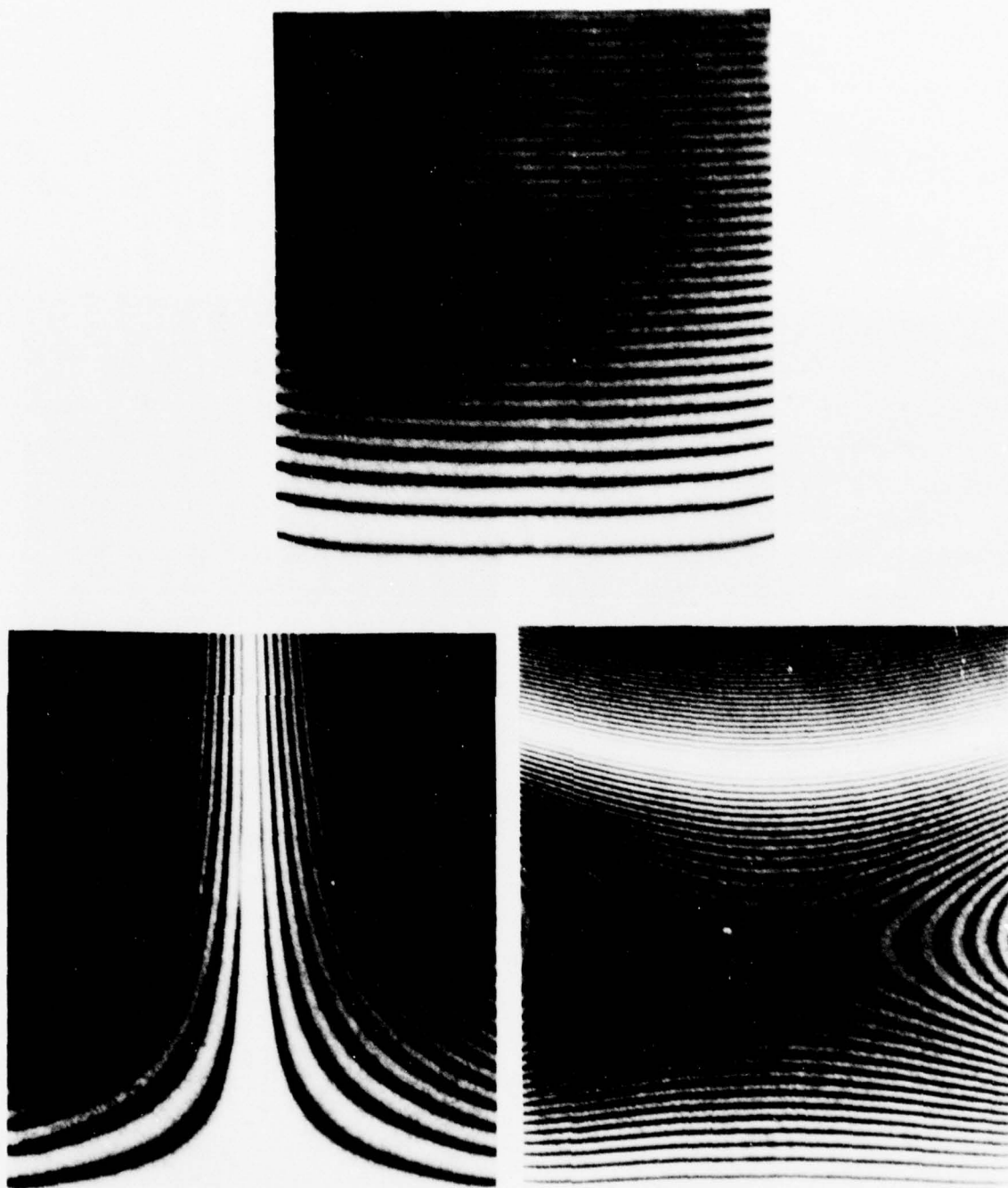


Figure 3 Photographs of the Holographic Reconstructions of the First Three Vibration Modes of a 0.330 cm. Thick Flat Cantilever Plate Excited at: (Top) 120.6 Hz, (Bottom Left to Right) 333.8 Hz and 730.6 Hz (Clamped Edge at Bottom)

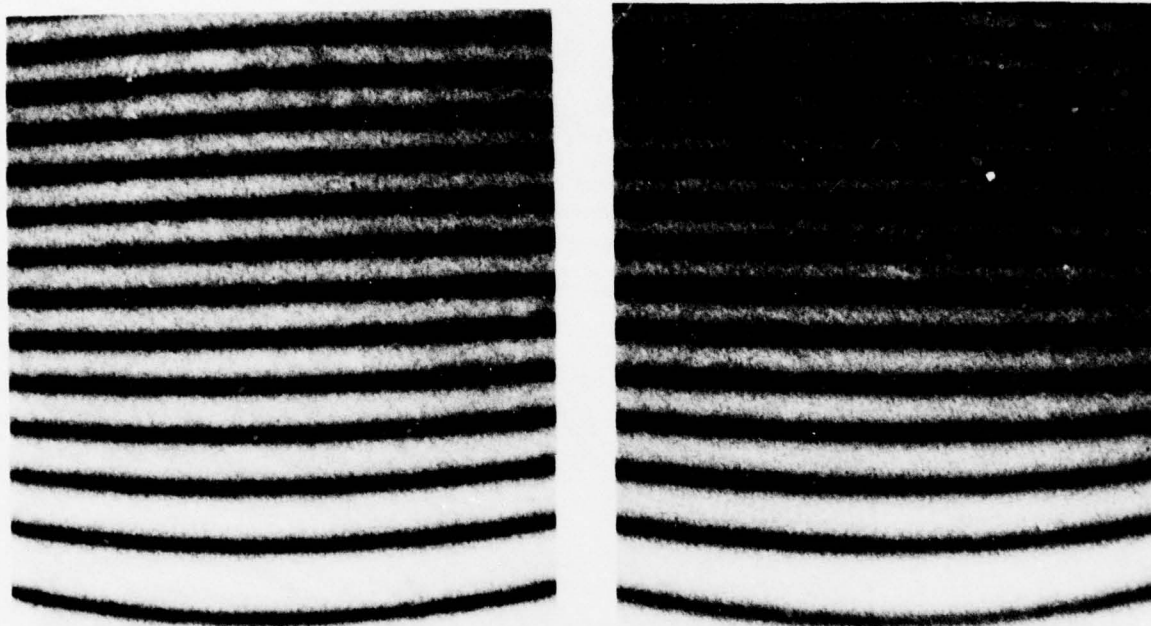


Figure 4a Photographs of the Holographic Reconstructions of the First Vibration Mode (806.0 Hz) of a 0.317 cm. Thick 45° Arc of a Cylindrical Shell with Object Beam Illumination from the Left and Right (Clamped Edge at Bottom)

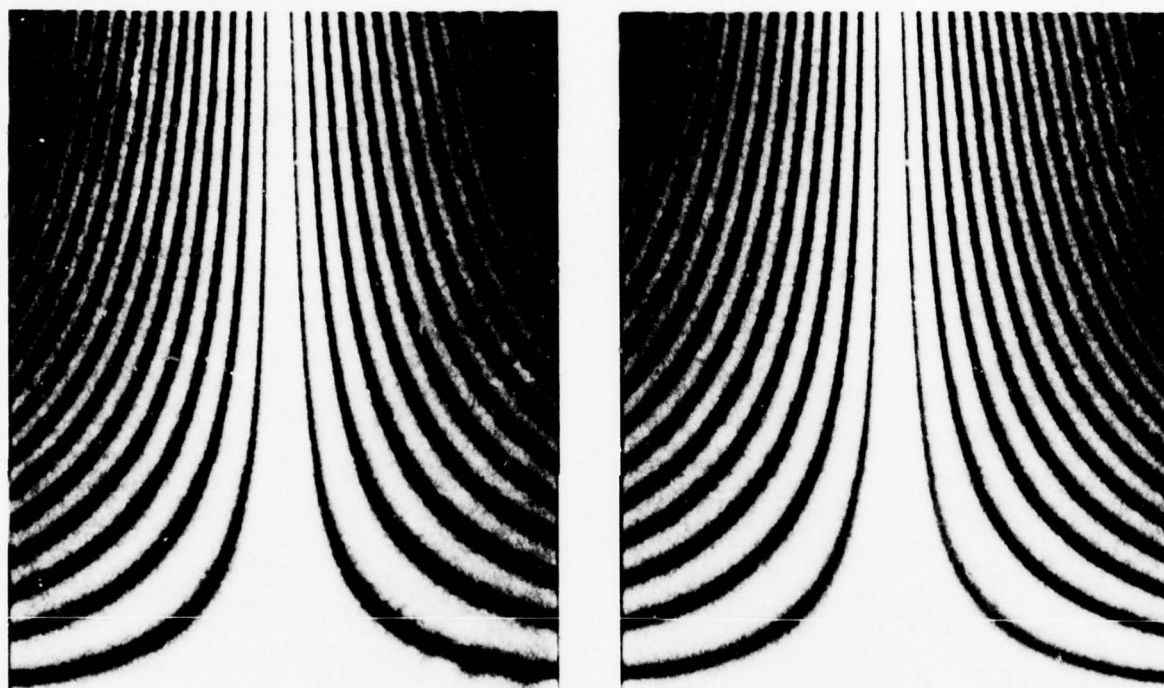


Figure 4b Photographs of the Holographic Reconstructions of the Second Vibration Mode (1380.0 Hz) of a 0.317 cm. Thick 45° Arc of a Cylindrical Shell with Object Beam Illumination From the Left and Right (Clamped Edge at Bottom)

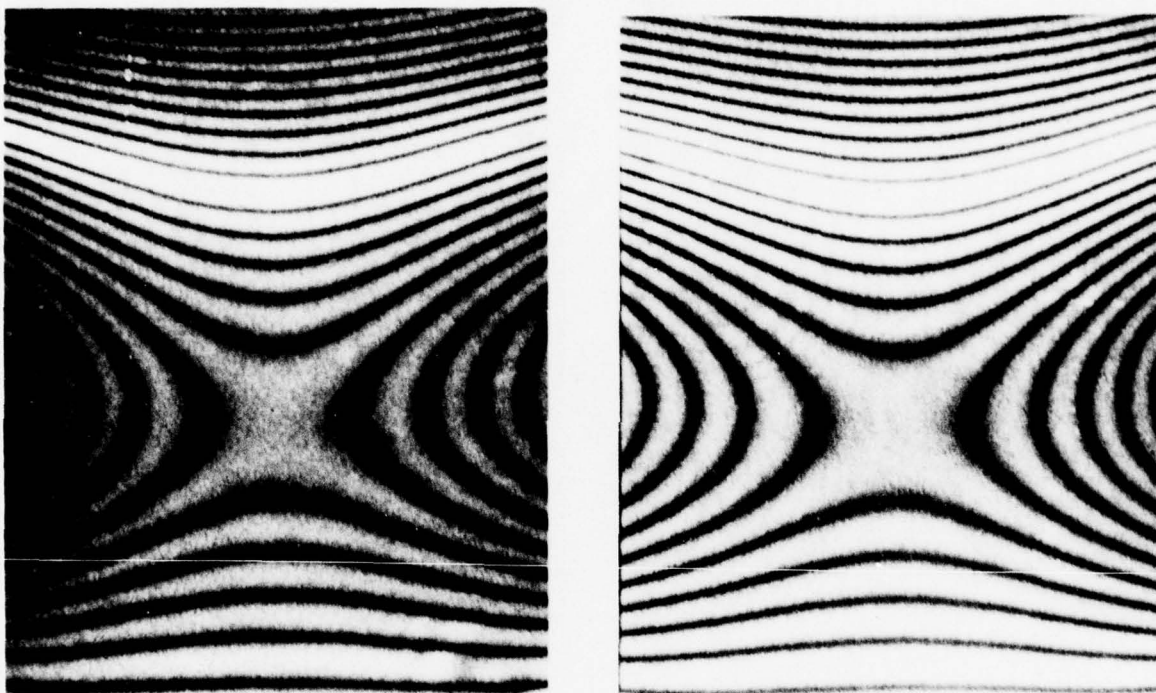


Figure 4c Photographs of the Holographic Reconstructions of the Third Vibration Mode (4080.0 Hz) of a 0.317 cm. Thick 45° Arc of a Cylindrical Shell with Object Beam Illumination From the Left and Right (Clamped Edge at Bottom)

reconstructions were digitized using sections whose centers corresponded to sixteen of the NASTRAN grid points. The holographic data was processed to obtain vectorial displacements (Ref. 6) (under the assumption that motion in the axis of the cylinder was negligible). Table III shows the comparison between the NASTRAN and holographic results for the first three modes of the shell.

TABLE II
MODE FIT DIFFERENCES: NASTRAN VS. HOLOGRAPHY

Differences in		TABLE IV					
Mode 1		.0005	.0036	.0024	.0032	.0027	.0031
Mode 2		-.0045	-.0010	-.0019	-.0055	.0061	.0109
Mode 3		.0246	.0202	.0206	.0233	.0224	.0323
		.0044	.0061	.0040	.0030	.0023	-.0011
		.0080	.0003	-.0050	.0014	.0155	.0150
		.0290	.0210	.0180	.0190	.0260	.0300
		.0060	.0060	.0060	.0030	.0020	.0020
		.0040	-.0040	-.0104	.0161	.0230	.0200
		-.0030	-.0070	-.0030	.0010	.0120	.0240
		.0040	.0030	.0040	.0080	.0090	.0030
		.0010	-.0120	-.0296	.0200	.0280	.0270
		-.0280	-.0310	-.0150	-.0240	-.0150	.0000
		.0010	.0010	.0020	.0030	.0120	.0010
		.0000	-.0190	-.0110	.0190	.0270	.0140
		-.0410	-.0389	-.0290	-.0395	-.0282	-.0320
		-.0020	.0080	.0060	.0010	-.0030	-.0060
		.0050	-.0130	-.0070	.0190	.0280	.0190
		.0320	.0510	.0490	.0270	.0320	.0320

System Checks

The next computations involved the orthogonality checks and Rayleigh quotient checks. The former measure the degree to which the stiffness functions between modes are orthogonal, and the latter measure the ratio of maximum potential to maximum kinetic energy during the vibration cycle of a mode (Ref. 6). The orthogonality parameters should be zero and the Rayleigh quotients should be unity. These results are presented in Table IV.

TABLE III

NASTRAN RESULTS VS HOLOGRAPHIC RESULTS

Mode 1 - Axial	-.01895	-.01619	-.01822	-.01303
- Transverse	-.00178	-.00388	.00825	-.02961
Mode 2 - Axial	.02210	.00817	-.01030	-.02628
- Transverse	-.00660	-.01436	-.00388	.00896
Mode 3 - Axial	-.05821	-.07816	-.07416	-.06013
- Transverse	.02875	.01197	.00751	-.01111
	-.00748	-.01698	-.01624	-.00366
	-.01805	-.01758	-.01697	-.03012
	.02887	.00723	-.01140	-.02722
	-.02660	-.02838	-.01856	-.02402
	.02735	-.07566	-.07890	.03521
	.07074	.01388	-.00668	-.07456
	.00435	-.00302	-.00279	.00486
	-.01674	-.02101	-.03397	-.03059
	.00471	.00531	.00234	-.00915
	-.04948	-.03304	-.04546	-.05477
	.12680	-.04957	-.04852	.11050
	.06948	.00690	-.00592	-.00914
	.00738	.00514	.00022	.01026
	-.00242	-.02374	-.02121	-.03582
	-.00114	.00162	.01154	.01776
	-.06128	-.06014	-.07552	-.05538
	.03647	-.05390	-.05409	.12700
	-.17110	.04581	.01348	-.04418

TABLE IV

ORTHOGONALITY AND RAYLEIGH QUOTIENT CHECKS

Mode Index (nk)	Orthogonality Parameter		Rayleigh Quotient	
	Plate	Shell	Plate	Shell
1, 2	-.01141	-.000004		
1, 3	-.00019	+.085832		
2, 3	+.00309	.000000		
1, 1			1.0735	1.0282
2, 2			1.1047	1.0245
3, 3			1.1082	1.0852

Structural Redesign and Correlation

The next two tasks were to redesign the structures and evaluate the results via a second NASTRAN analysis. Both the cantilever plate and the cylindrical shell segment were redesigned subject to four constraints: a) lowering of the first mode frequency by 5 percent ($\Delta\omega_1/\omega_1 = -.049$); (b) raising of the second mode frequency by 5 percent ($\Delta\omega_2/\omega_2 = +.051$); (c) an admixture coefficient of the first to the second mode of magnitude 0.125 ($C_{21} = \pm .125$); and (d) an admixture coefficient of the third to the second mode of magnitude 0.025 ($C_{23} = -.025$). (For the plate the C_{21} parameter was positive, and for the shell it was negative. These sign conventions were necessary to generate the same shift in the node line of the second mode on both the plate and the shell and they resulted only from a change in the sign conventions between the NASTRAN analyses of the plate and the shell.) The results provided structures which could be fabricated, and which had root-mean-square thickness changes of 12.7 percent for the plate and 14.5 percent for the shell.

The new designs, as arrays of the fractional changes in thickness of the triangular elements of the plate and shell, respectively, are presented in Figs. 5a and 5b.

The designs of Figs. 5a and 5b were analyzed by NASTRAN to determine the new frequencies and mode shapes of these structures. The modes of the original structures were then used to form a series to approximate (to least-square-error) the shape of the new second mode, and therefore to give the resulting admixture coefficients C_{21} and C_{23} .

The final results are presented in Table V, together with the results predicted by the more accurate perturbation calculation mentioned earlier in the description of the CHANGNAST program, and considered further in Appendix.

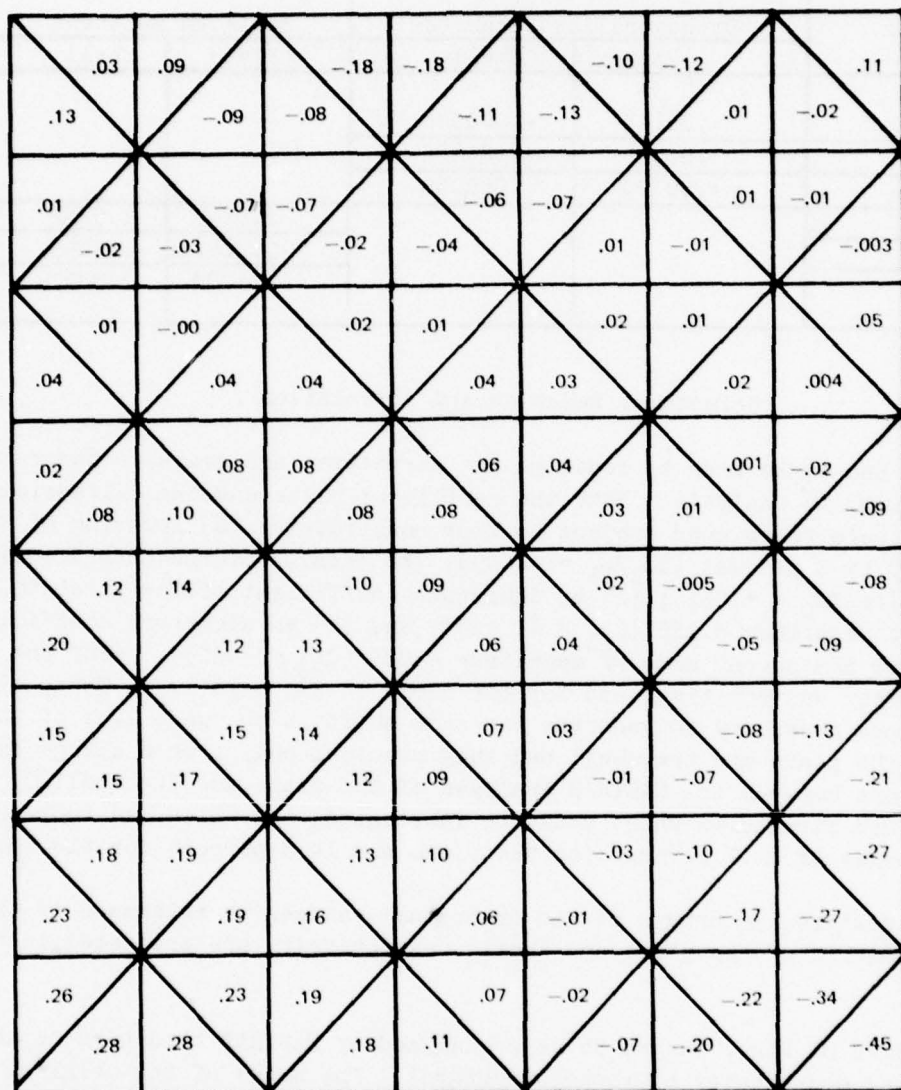


Figure 5a New Design for the Flat Plate, Presented as a Ratio of the Change in Thickness ($\Delta h/h$) for Each of the Elements (Clamped Edge at Top)

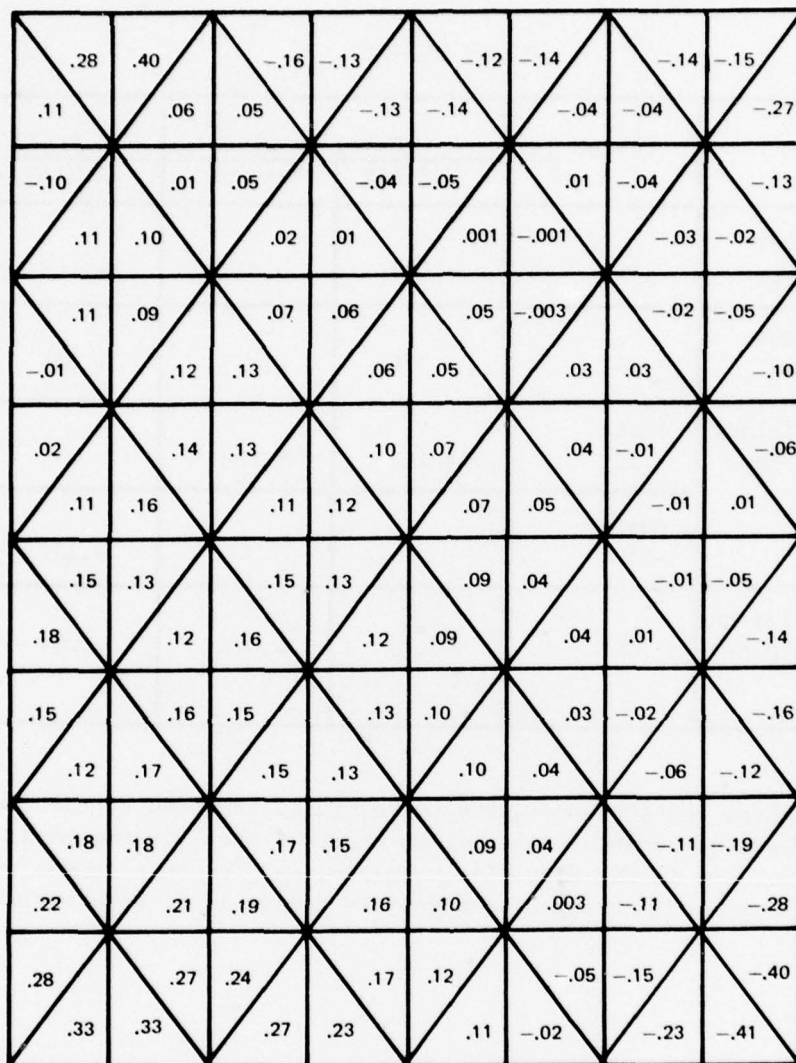


Figure 5b New Design for the 45° Arc of a Cylindrical Shell as a Ratio of the Change in Thickness ($\Delta h/h$) for Each of the Elements (Clamped Edge at Top)

TABLE V

FINAL RESULTS

Constraint	Design	Plate Results		Shell Results	
		NASTRAN	Perturb.	NASTRAN	Perturb.
Change in 1st Mode Frequency, $\Delta\omega_1/\omega_1$	-.049	-.027	-.037	-.042	-.041
Change in 2nd Mode Frequency, $\Delta\omega_2/\omega_2$	+.051	+.076	+.067	+.084	+.079
Admixture Coefficient 1st Mode to 2nd Mode C_{21}	Plate +.125	+.102	+.124		
	Shell -.125			-.112	-.118
Admixture Coefficient 3rd Mode to 2nd Mode C_{23}	-.025	-.021	-.026	-.027	-.028

The mode shape changes were quite successfully rendered by the new design. However, the frequency changes have fallen short of what was required. All the changes, however, are in the direction required, and for this reason we may expect that the process would converge upon a desired design if it were applied iteratively.

SECTION VI

CONCLUSIONS AND RECOMMENDATIONS

Under the present contract, it was shown that it is feasible to apply the inverse perturbation design method, originally developed at United Technologies Research Center (Refs. 4 and 5), directly to the output of a finite element computer analysis of a structure. Thus, this new structural design tool, at first limited to a very simple geometry whose response characteristics could be sufficiently characterized without the help of a NASTRAN type computation, has the potential for application to the mathematically complex structure of, for example, a turbine blade. (The twist and camber of such structures create analytical difficulties requiring the use of finite element analysis to calculate their vibration modes to the necessary accuracy.) As described in the previous section, the initial step in this direction has been taken with the redesign of a shell shaped cantilever beam. In addition, the methodology was also applied to the redesign of a flat cantilever plate for comparison with previous work, described in the Appendix to the present report, which only required vibration data obtained holographically.

There is, of course, additional development required and, consequently, it is recommended that the work be extended to permit refinement of the analytical approach, together with experimental investigations concerned with the fabrication and test of a redesigned structure. Further, attention needs to be devoted to the inclusion of additional, permissible physical design changes other than the single parameter of thickness, to which the technique has been restricted to date.

In summary, continued development of the inverse perturbation design procedure would set the stage for: a) redesigning actual turbine blades; b) carrying out iterative design procedures without the need for fabricating intermediate prototypes; c) introducing holographic data into NASTRAN analyses to improve computer modeling of turbine blades and other structures; and d) using holographic data itself, rather than NASTRAN output, for the inverse perturbation design of structures.

APPENDIX

REDESIGNING STRUCTURAL VIBRATION MODES BY INVERSE PERTURBATION, SUBJECT TO MINIMAL CHANGE THEORY*

Abstract

If first-order perturbation theory for the vibration modes of a structure is to be inverted so as to design a new structure having desired changes in vibration modes, it is essential to keep the structural changes as small as possible. This not only helps keep the changes within the approximation of first-order perturbation analysis, but also avoids ill-conditioning of the simultaneous equations that must be solved for a new design. Calculus of variations may be used to find the minimal changes, and specifies a unique set of functions, derived from pairs of vibration modes, that are optimal for expressing the structural changes needed to accomplish a given set of changes in vibration modes. This theory is put into practice for a cantilever plate, for which vibration-mode data is obtained by holographic vibration analysis.

Introduction

Two previous papers (Refs. 4 and 5) have outlined both a general first-order perturbation theory for the vibration modes of a structure and the inversion of that theory for the purpose of structural redesign. Specifically, the first answered the question: How will a small change to a structure, whose vibration modes are known, affect those vibration modes? The second answered the question: How should a structure, whose vibration modes are known, be modified to alter certain modes? The use of first-order perturbation theory to answer the first question may not be practical because finite-element computer analyses can often provide such answers more accurately. This is because first-order approximations often become more error prone in vibration theory than modeling approximations by finite elements. With the second question, however, perturbation methods may have an advantage if a considerable number of simultaneous changes to vibration modes are required. This is because the computation time required for finite-element analyses can make hunt-and-try methods impractical. Still, dependence upon first-order variational theory of vibration modes can make an inverse-perturbation design procedure quite inaccurate unless the structural changes are kept small. A method is needed, therefore, to find the smallest physical change to a structure that will alter its vibration modes in the desired manner.

* This appendix was authored by K. A. Stetson, I. R. Harrison and G. E. Palma.

The next section of this appendix presents an application of the calculus of variations to the problem of finding the minimum structural change necessary to achieve a desired set of changes in the vibration modes. The remainder of the appendix deals with the application of this theory to the redesign of a cantilever plate, based upon data acquired by holographic vibration analysis. The design parameter permitted to vary was the thickness of the plate, although, in principle, the length and breadth of the plate could be used as design variables also. This application required the development of both: 1) the necessary computer program to perform the inverse perturbation design routine; and 2) a program to analyze holographic interferograms of vibration modes so as to obtain accurate second derivatives of the normal mode functions. These latter were required to model the changes in bending strain due to changes in plate thickness. In the end, new designs were actually generated and built as cantilever plates of nonuniform thickness. These new plates were then analyzed to compare the actual changes in normal vibration modes with the changes prescribed.

Theory

Minimization of Inverse Perturbation

The perturbation theory, as presented in Ref. 4 can be summarized as follows. Let us assume that a small, distributed change, $f(x)$, is made to a structure. For every pair of vibration modes of the structure, $\phi_n(x)$ and $\phi_k(x)$, there exists a function, $\theta_{nk}(x)$, which describes the effect the change will have on these modes by the integral

$$\Delta_{nk} = \int_0^L \theta_{nk}(x) f(x) dx. \quad (1A)$$

The variable x is taken to represent one, two or three dimensions depending upon the nature of the structure, and L and 0 denote its boundaries. The parameter, Δ_{nk} , describes change in either the square of the natural frequency if $n=k$, or admixture between modes if $n \neq k$, i.e.,

$$\Delta_{nn} = \Delta\omega_n^2/\omega_n^2, \text{ and } \Delta_{nk} = C_{nk}(\omega_n^2 - \omega_k^2)/\omega_n\omega_k, \quad (2A)$$

where ω_n and ω_k are the natural frequencies (in radians) of the n th and k th modes, and C_{nk} is the admixture coefficient that describes the amount of the ϕ_k modeshape that the ϕ_n mode subsumes as a result of the structural change. The mode admixture is described by

$$\phi'_n(x) = \phi_n(x) + \sum_k C_{nk} \phi_k(x) \quad (3A)$$

where $\phi'_n(x)$ is the new shape of mode ϕ_n , and $k=n$ is omitted from the summation. The functions, $\phi_{nk}(x)$, which may be called perturbation functions, need not be explicitly defined at this point.

In redesigning the structure, we wish to specify certain changes in modal frequencies $\Delta\omega_n$, and certain changes in mode shapes expressible by admixture coefficients C_{nk} ; these changes specify certain Δ 's via Eq. (2A). The goal, of course, is to find a suitable function $f(x)$, which will yield these Δ 's via Eq. (1A). Unfortunately, there may exist a wide choice of functions that all yield these Δ 's. Let us seek, however, to find that function which will make the minimum change to the structure. If we follow the procedure outlined by Schultz and Melsa (Ref. 7), we first require a suitable index of the change to the structure; for example, the integral of the square of $f(x)$. This may be referred to as a functional of the function, $f(x)$, in that for any given function, the functional takes on a given value. If the variation of the functional exists and the functional takes on a minimum for a given function, then the variation of the functional will be zero for that function. We seek, therefore, a function that will satisfy the condition

$$\delta \int_0^L f^2(x) dx = 0. \quad (4A)$$

However, we also want the function to yield a given set of Δ 's via a given set of Eqs. (1A), i.e., when integrated times a given set of perturbation functions, $\phi_{nk}(x)$. These conditions are constraints upon our choice of functions, $f(x)$. They may be introduced into Eq. (4A) by the technique of undetermined multipliers. Let us use the index p for the mode pair nk , and express the constraints in the following form:

$$0 = \int_0^L [\Delta_p/L - \phi_p(x)f(x)] dx \quad (5A)$$

Let us assume that we have specified a set of P constraints as our goal for redesign of the structure. Since each of the P Eqs. (5A) equals zero, we may multiply each by an arbitrary factor, $2\lambda_p$, and add it to Eq. (4A) without changing the variance of the functional. This gives

$$\delta \int_0^L \{f^2(x) + 2\sum_1^P \lambda_p [\Delta_p/L - \phi_p(x)f(x)]\} dx = 0. \quad (6A)$$

Since the variational equation is in the form

$$\delta \int_0^L \mathcal{X}(f(x), x) dx = 0,$$

we are led to the Euler equation

$$\partial \mathcal{X} / \partial f = 0. \quad (7A)$$

This leads to the solution for the desired function, $f(x)$,

$$f(x) = \sum_1^P \lambda_p \theta_p(x). \quad (8A)$$

The perturbation functions take on an interesting role in this problem in that they not only may be used to determine the effects of any structural changes, they themselves form a set of optimal functions for formulating changes to the structure.

To determine the coefficients of the series in Eq. (8A), the λ_p 's, substitute for $f(x)$ in Eq. (1A).

$$\Delta_p = \sum_1^P \lambda_p \int_0^L \theta_p(x) \theta_q(x) dx. \quad (9A)$$

There are P such equations each of which has P unknown λ 's, for which we may solve by the matrix equation

$$(\lambda) = [\Psi]^{-1} (\Delta), \quad (10A)$$

where the elements of Ψ , which may be called the perturbation matrix, are

$$\Psi_{pq} = \int_0^L \theta_p(x) \theta_q(x) dx. \quad (11A)$$

(Parentheses denote vectors or single column matrices and square brackets matrices.) The final structural change may be expressed by

$$f(x) = (\Delta)^T [\Psi]^{-1} (o(x)). \quad (12A)$$

If the perturbation functions are independent over the boundaries of the structure, it can be shown (Ref. 8) that the matrix generated by Eq. (11A) must be nonsingular. In general, the perturbation functions are independent even though they are not orthogonal. This is true even if complementary pairs of perturbation functions, ϕ_{nk} and ϕ_{kn} , are included, because these functions are not proportional unless pure mass or pure stiffness changes are made. The rank of the perturbation matrix is determined solely by the number of constraints, or redesign changes, required, and not by the number of degrees of freedom of the structure. This generally means that the perturbation matrix will not be very large.

Formulating the problem, as above, allows one further insight into the process of structural redesign. It is quite easy to show that the absolute minimum root-mean-square change to the structure needed to accomplish a suggested redesign is

$$\text{Min} \left\{ \int_0^L f^2(x) dx \right\}^{1/2} = \{ (\Delta)^T [\Psi]^{-1} (\Delta) \}^{1/2} \quad (13A)$$

This gives a measure of the difficulty involved in making any suggested change in the vibration modes of a structure. It will not, however, indicate any specific violations of physical reality, such as negative plate thicknesses.

Application to Plate Design

For an isotropic plate, whose thickness we may vary, we may (as in Ref. 4) write the following expression for the change parameter, Δ_{nk} ,

$$\Delta_{nk} = (\omega_n \omega_k M_k)^{-1} \iint [(\phi_k'')^T G(\phi_n'')((1+\Delta h/h)^3 - 1) - \omega_n^2 \rho h \phi_n \phi_k \Delta h/h] dx dy. \quad (14A)$$

M_k is the modal mass of the k th mode, defined by

$$M_k = \int \rho h \phi_k^2 dx dy, \quad (15A)$$

where ρ is the volume density of the material, and h is the plate thickness. In Eq. (14A), Δh is the change in plate thickness and (ϕ_n'') is defined by

$$(\phi_n'') = \begin{pmatrix} \phi_n^{xx} \\ \phi_n^{yy} \\ \phi_n^{xy} \end{pmatrix}, \quad (16A)$$

where superscripts denote partial differentiation with respect to the superscript variables, and G is defined by

$$G = \begin{bmatrix} 1 & \nu & 0 \\ \nu & 1 & 0 \\ 0 & 0 & 2(1-\nu) \end{bmatrix} E h^3 / 12(1-\nu^2), \quad (17A)$$

where E is Young's modulus and ν is Poisson's ration. $(\phi_k'')^T$ denotes the transpose of the column matrix, formed for the k th mode, as defined in Eq. (16A). The percentage change in frequency of a mode and the admixture coefficients between modes may be calculated from the change parameters by

$$\Delta\omega_n/\omega_n = (1 + \Delta_{nn})^{1/2} - 1, \text{ and} \quad (18A)$$

$$C_{nk} = \Delta_{nk} \omega_n \omega_k / (\omega_n^2 - \omega_k^2). \quad (19A)$$

To put Eq. (14A) into the form of Eq. (1A), we must obtain $\Delta h/h$ (the percentage change in thickness) as a common factor of both terms in the integrand. This can be done by taking the first-order approximation

$$((1 + \Delta h/h)^3 - 1) \approx 3\Delta h/h. \quad (20A)$$

From this, the perturbation function becomes

$$\theta_{nk} = (\omega_n \omega_k M_k)^{-1} [3(\phi_n'')^T G (\phi_k'') - \omega_n^2 \rho h \phi_n \phi_k]. \quad (21A)$$

This is the function that may be used in Eqs. (11A) and (12A) with $\Delta h/h$ replacing $f(x)$.

The use of approximation (20A) yields a design procedure that makes design changes that accurately model changes in mass, but only approximately model changes in stiffness. Alternatively, we could choose linear changes in the cube of thickness, $\Delta(h^3)/h^3$, as our structural change, $f(x)$, and perform the approximation in the second term of the integrand of Eq. (14A). This leads to a perturbation function that is simply 1/3 the value of that in Eq. (21A). Thus, we may consider either of two possibilities for the redesign of an isotropic plate based on exact changes in mass, $(\Delta h/h)_m$, or on exact changes in stiffness, $(\Delta h/h)_s$. The two are related by

$$(\Delta h/h)_s = (1 + 3(\Delta h/h)_m)^{1/3}. \quad (22A)$$

Ideally, it would be desirable to make design changes that were modeled exactly in both mass and stiffness. Attempting to do this leads to an Euler equation that cannot be solved meaningfully in the simple form of Eq. (8A). Nonetheless, once a design has been obtained, Eq. (14A) can be used to generate a more exact estimate of the values of Δ_{nk} to be expected.

Experimental Application

General Considerations

In choosing an experimental application of the proposed design technique, we considered the following: There was considerable interest in a method that could function with experimentally determined data, specifically, holographically obtained data. There was interest in structures that resembled turbine blades; however, for simplicity, we preferred to work with a plate structure. This led to the choice of a cantilever plate. Holographic vibration analysis would provide displacement data for the vibration modes which would require numerical processing to obtain second derivatives. Errors in displacement data generally lead to severe errors in computation of second partial derivatives. Since our second partial derivative functions were to be integrated, to form a perturbation matrix, or to model distributed changes in the thickness of the plate, the average value of the second partials over segments of the plate would be more important than their peak values. (The latter are more important for prediction of failure due to stress.) This led to the idea of dividing the plate into sections, fitting the data within each section to a bi-quadratic function by least-square-error theory, and differentiating this function to obtain the average value of the second derivative. Furthermore, there would be similarities between this approach and the approach we would have to take if we were to use vibration modes computed by finite element analyses as our input.

MODES Program

A computer program, named MODES, was written to obtain the second partial derivatives of the modes of a plate. The program accepts data, in the form of x and y coordinates and a fringe number, from photographs of holographic reconstructions of the mode functions. It then fits this mode data for least-square error to a quadratic function of two coordinates.

Because the second partial derivatives are required for the computation of the perturbation functions, the mode shape must fit, to lowest order, a quadratic function in two dimensions. A bi-quadratic, rather than a bi-cubic fit, is used in order to simplify the subsequent calculations, and to minimize the data error. A cubic fit would follow the data errors more closely because of its added degrees of freedom. The bi-quadratic function used may be expressed as

$$\phi = Ax^2 + By^2 + Cxy + Dx + Ey + F, \quad (23A)$$

where ϕ is the mode value at any point x, y and $2A$ is the second partial derivative with respect to x, ϕ^{xx} ; $2B$ is the second partial derivative with respect to y, ϕ^{yy} ; and C is the cross partial derivative, ϕ^{xy} . D and E are the average first-partial derivatives with respect to x and y, respectively, and F is the average value over the section.

We are approximating a mode function of a structure which has continuous and smooth first and second partial derivatives. Whereas the vibration amplitude represented by a fringe is exact, there is error encountered in locating the center of a fringe. In order to minimize the effect of this error, we must average over the data. In this process, the fewer the degrees of freedom, the more the error effect is minimized, which is why the data is fit to a bi-quadratic, which has constant second partial derivatives. Because the fit to the vibration data yields constant second partial derivatives over the area considered, it is necessary to analyze the structure in sections, which gives an average fit for each section of the mode. The constraint that the total function be continuous between sections could be added, and a solution obtained; however, doing this makes the computation more complex since the fits for all sections must be solved simultaneously. For simplicity, data from each section of the structure was fit independently, and continuity sacrificed. To get a good approximation to the mode function without the continuous and smooth boundary constraints between sections, many sections should be used. We must strike a balance, however, between getting a good, smooth overall fit to the mode, and getting enough data per section to minimize data error. This was done empirically by recording holograms with high fringe densities and dividing the structure so that at least fifty data points could be taken per section.

After the data from each section of the structure has been fit to a bi-quadratic function, a computer storage file is formed for each mode, with the coefficients of the particular mode fit and the center coordinates for each section of the structure stored in that file.

In actual use, the program was run on a time-sharing computer terminal and a mode file name and fringe-order type were chosen. For each section, data was entered as an x-y position and fringe number. A coordinate shift was made on each set of data points, relative to the center of the section. Each data point, and its corresponding fringe-order value, were used to compile matrix coefficients, the contributions to which were linearly additive for each data point. After adding the term for that point into the matrix, each data point is discarded as the next point is read. The matrix and the vector, formed and solved for each section are

$$\begin{bmatrix} A \\ B \\ C \\ D \\ E \\ F \end{bmatrix} = \begin{bmatrix} \Sigma x_n^4 & \Sigma x_n^2 y_n^2 & \Sigma x_n^3 y_n & \Sigma x_n^3 & \Sigma x_n^2 y_n & \Sigma x_n^2 \\ \Sigma x_n^2 y_n^2 & \Sigma y_n^4 & \Sigma x_n y_n^3 & \Sigma x_n y_n^2 & \Sigma y_n^3 & \Sigma y_n^2 \\ \Sigma x_n^3 y_n & \Sigma x_n y_n^3 & \Sigma x_n^2 y_n^2 & \Sigma x_n^2 y_n & \Sigma x_n y_n^2 & \Sigma x_n y_n \\ \Sigma x_n^3 & \Sigma x_n y_n^2 & \Sigma x_n^2 y_n & \Sigma x_n^2 & \Sigma x_n y_n & \Sigma x_n \\ \Sigma x_n^2 y_n & \Sigma y_n^3 & \Sigma x_n y_n^2 & \Sigma x_n y_n & \Sigma y_n^2 & \Sigma y_n \\ \Sigma x_n^2 & \Sigma y_n^2 & \Sigma x_n y_n & \Sigma x_n & \Sigma y_n & N \end{bmatrix}^{-1} \begin{bmatrix} \Sigma \Omega_n x_n^2 \\ \Sigma \Omega_n y_n^2 \\ \Sigma \Omega_n x_n y_n \\ \Sigma \Omega_n x_n \\ \Sigma \Omega_n y_n \\ \Sigma \Omega_n \end{bmatrix} \quad (24A)$$

where the letters A through F are coefficients of the fitted polynomial in Eq. (1A), x_n and y_n are the coordinates of the data point of the fringe whose order generates the value Ω_n , and N is the total number of data points. After sufficient data has been entered for a section, the user types END, which signals the computer to solve for the coefficients A through F of Φ_n . This process is repeated for each section of the structure, and all sections are included in the mode fit file.

Testing the MODES Program

The MODES program was tested for its accuracy in calculating second derivatives, and its sensitivity to data error by taking data from a known mode function which was not of quadratic form. The data was generated numerically from an analytical function, and these values were used in the mode fitting program. Then, random error was added to the data and the sensitivity to the error was determined.

The theoretical solution for a plate, hinged at all edges, was used for this test. The two vibration modes were

$$\begin{aligned}\phi_1 &= \sin(x) \sin(y), \text{ and} \\ \phi_2 &= \sin(x) \sin(2y) .\end{aligned}\tag{25A}$$

Contour plots of these modes are shown in Fig. 1A. The first quadrant of this plate was divided into 25 sections, and the data from these sections were used in the MODES program. The exact values of the second partial derivatives, averaged over a section, and the exact values, calculated at the center point, were computed from the analytical equations. Random error was then added to the same data and used in the MODES program. (The error was added to the fringe values, although the actual error occurs in the x-y values, because the real error occurs as a percentage of the fringe spacing and varies in size from fringe to fringe. So long as the error is small, this can be approximated by an error of uniform size in the fringe values.) Different percents of error were tested, and the results (shown in Table IA) indicate that less than 5 percent error is desirable.

TABLE IA
RANDOM ERROR EFFECTS ON MODES PROGRAM

Sect. 1	1 percent	5 percent	10 percent
ϕ^{xx}	-.0845	-.0877	-.0321
ϕ^{yy}	-.1139	-.0696	-.349
ϕ^{xy}	+.9077	+.8955	+.8589
Sect. 2			
ϕ^{xx}	-.1843	-.2581	-.3508
ϕ^{yy}	-.1842	-.1135	-.0957
ϕ^{xy}	+.7247	+.7261	+.5735
Sect. 3			
ϕ^{xx}	-.0715	-.0365	-.1099
ϕ^{yy}	-.0695	-.0558	-.1479
ϕ^{xy}	+.6188	+.6058	+.6636

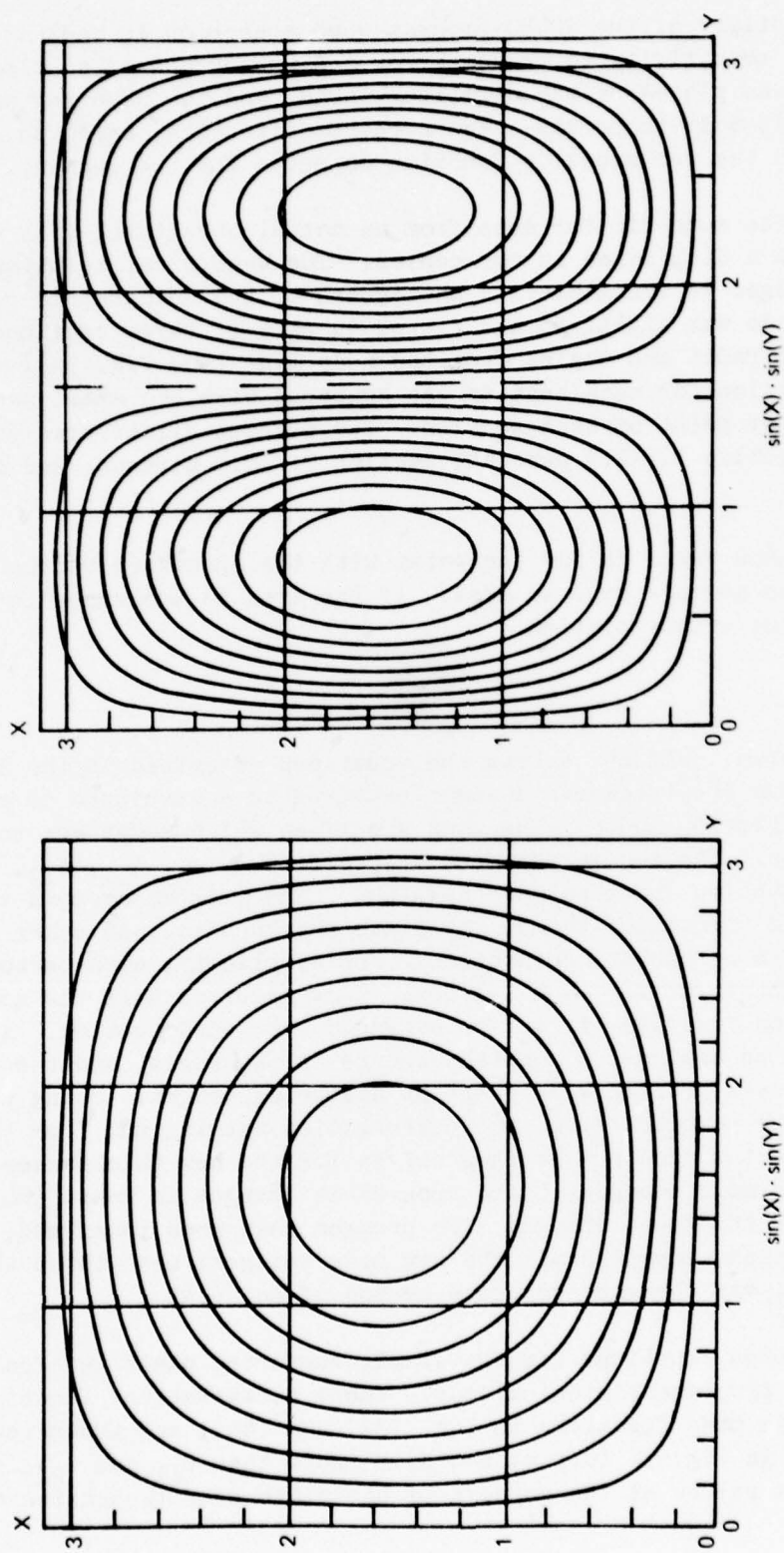


Figure 1A Contour Plots of the First Two Modes of a Simply-Supported Square Plate

The repeatability of the MODES program when a section is redigitized is also a measure of its sensitivity to random error. A photograph of a holographic vibration mode was placed on the digitizer table, and the same region was digitized several times. At most there was a two percent difference, based on successive digitizations, in the perturbation function computed for the segment.

To compare the mode fit for data from an actual structure, with an analytical solution, we used a disk fixed in the center. The analytical solution for a circular disk with free edges is available. A photograph of the holographic reconstruction of a two diameter mode was digitized and fitted in each of three sections. The sections were at different radii and angles from the node line (see Fig. 2A). The calculated perturbation function for each section was compared with the exact analytical value at the center point of each section. The percent differences for each section were: section 1, 12.5 percent; section 2, 10.4 percent; and section 3, 26.0 percent.

Each calculated value is for the point with the specified radius and angle, and the mode fit is an average over an area. If the area is decreased in size, the fit should approach the exact solution.

CHANGES Program

Another program, CHANGES, solves the equations described in the section on Theory to calculate the thickness changes required in a structure to make desired changes in the vibration modes. The user specifies which modes are to be changed, and by what amount. The change parameters specified (i.e., Δ_{11} , Δ_{12} , etc.) determine which perturbation functions are required. The program accepts the mode coefficients (and normalizes them), the plate thicknesses, and other constants needed to form each perturbation function. For simplicity, each perturbation function has a constant value for each section. This requires that the modal component of the perturbation function, $\phi_n \phi_k$, be averaged over each section. As a result, each section will be assigned a constant change in thickness, and the new plate will have a thickness profile with steps of differing height. Using the perturbation functions, the computer forms the perturbation matrix, and from the change parameters, the vector of Δ 's. It then solves for the new thicknesses of a plate having the desired mode changes, based upon exact changes in mass, $(\Delta h/h)_m$, and prints out the RMS thickness change. The program then goes back, and, using the new plate thicknesses, computes all the new mode changes; even those where change was not specified, via the more accurate method of Eq. (14A).

The perturbation functions for the simply supported plate were calculated analytically on a programmable calculator. These perturbation functions were calculated for the two mode functions in Eqs. (3A) and (4A), and the perturbation functions can be seen in Fig. 3A (a,b,c, and d). (Note that ϕ_{11} and ϕ_{22} , for example, have their maximum values at the corners of the plate even though the mode functions

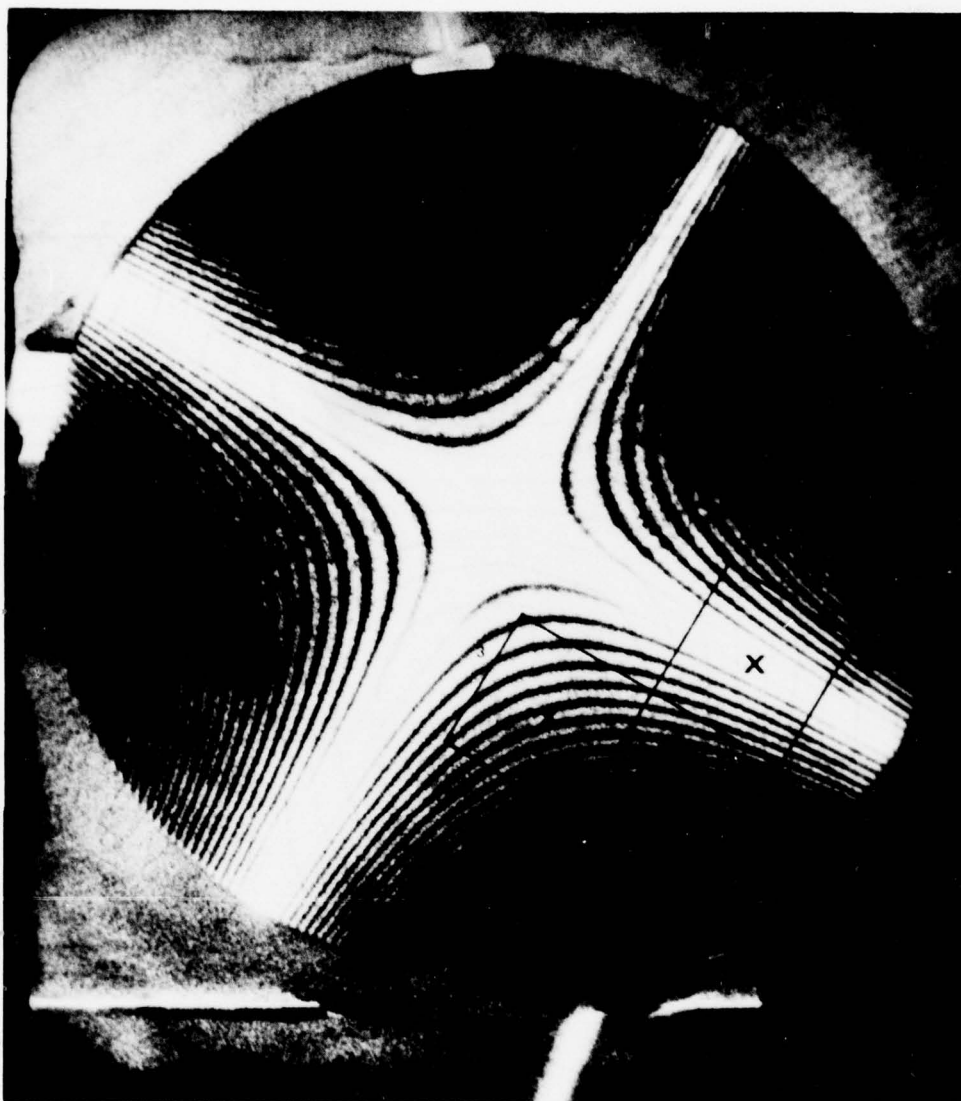


Figure 2A Photograph of a Holographic Reconstruction of a Circular Disk Vibrating in its First Two-Diameter Mode (Three Sections Indicate Where Data was Digitized)

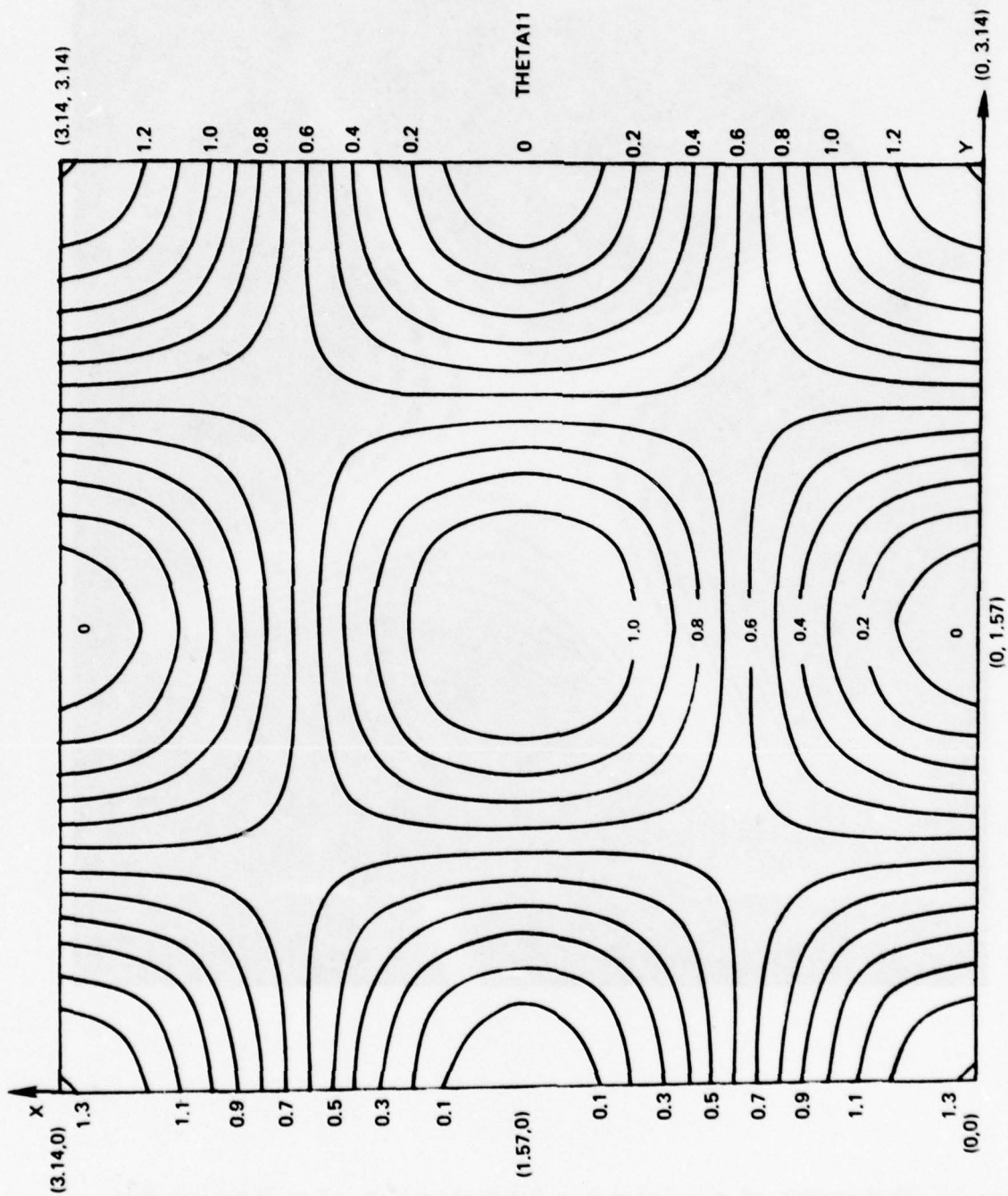


Figure 3Aa Analytically Calculated Perturbation Function of a Simply-Supported Square Plate Showing Contours of Constant Sensitivity to a Change in Thickness of the First Mode Frequency

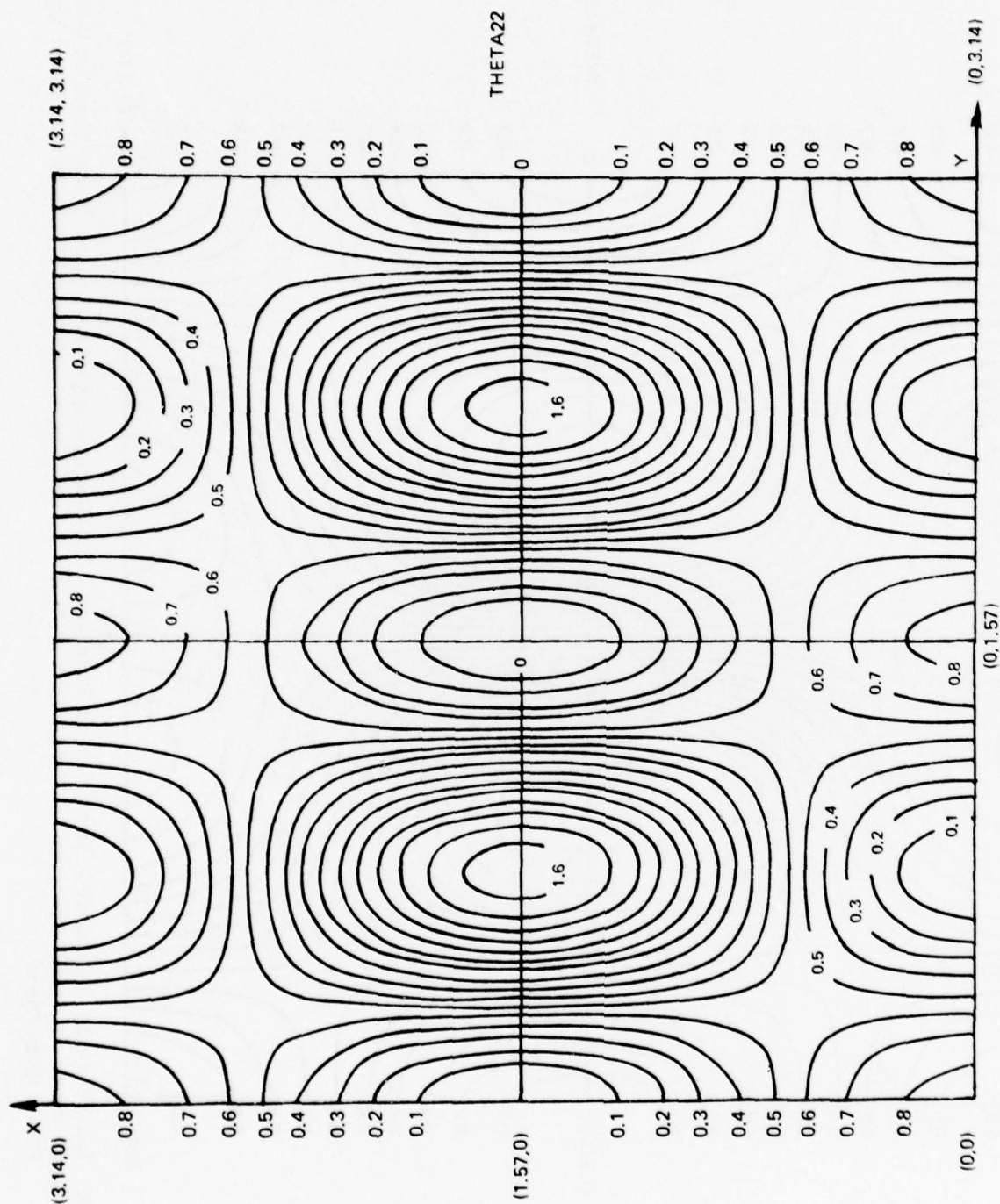


Figure 34b Analytically Calculated Perturbation Function of a Simply-Supported Square Plate Showing Contours of Constant Sensitivity to a Change in Thickness of the Second Mode Frequency

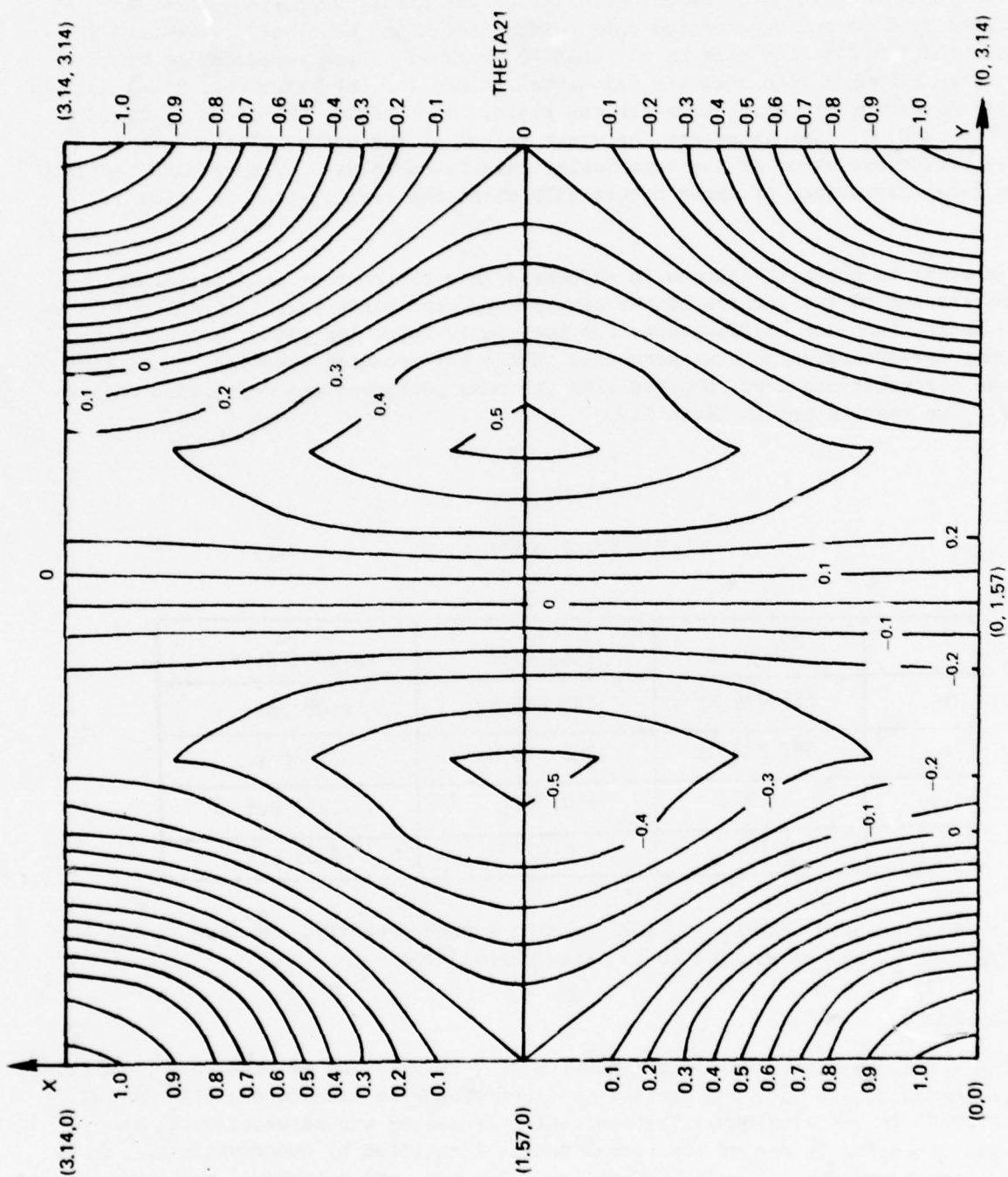


Figure 34d Analytically Calculated Perturbation Function of a Simply-Supported Square Plate Showing Contours of Constant Sensitivity to a Change in Thickness of the Amount of First Mode Shape Added to the Second Mode Shape

are zero there. This results from the high bending that occurs in the corners.) Next, the mode coefficients for one quadrant of the simply supported plate, as calculated from computer-generated data points (see MODES sections), were used in the perturbation function part of the CHANGES program. These perturbation function values were compared with computer calculated values for the exact analytical solution of the perturbation function for the plate. The results are shown in Fig. 4A (a,b,c, and d). Tabulated are the exact values at the center of the section and the percentage error of the numerically calculated values. The results indicate that a large percentage of error occurs only where the perturbation function is small.

In order to check if changes in thickness gave the correct mode perturbations, the thicknesses of two corners of the simply supported plate were thinned by 30 percent. Again, the mode coefficients for the simply supported plate, as calculated from computer-generated points, were used in the perturbation function. This time the mode perturbations were compared with the mode perturbations calculated analytically. The results are in Table IIA.

TABLE IIA
PERTURBATION COMPARISONS

	Computed	Analytic	Percent Diff.
ω_1	151.779 Hz	151.645 Hz	+0.08 pct.
ω_2	387.233 Hz	386.378 Hz	+0.22 pct.
C_{12}	+0.012923	+0.013311	-0.291 pct.
C_{21}	-0.01166	-0.01277	-8.69 pct.

It was concluded that the CHANGES program worked properly, and that it and the MODES program should be applied to an experimental test.

Implementation

The structure chosen for redesign was a 12.7 cm by 15.24 cm cantilever aluminum plate, clamped on one end, and excited by electromagnetic transducers stimulating eddy currents in the aluminum. The excitation frequency was adjusted until the plate was vibrating in one of its normal modes, identified by observation through a speckle interferometer. A suitable amplitude was set, and holograms were recorded for the first five modes, the first three of which were presented as Fig. 3 in the main body of the report. The frequency of the maximum response for each mode was recorded ($f_1 = 120.6$ Hz, $f_2 = 333.8$ Hz, $f_3 = 730.6$ Hz) and photographs were taken of each holographic reconstruction and enlarged prints made.

THETA 11

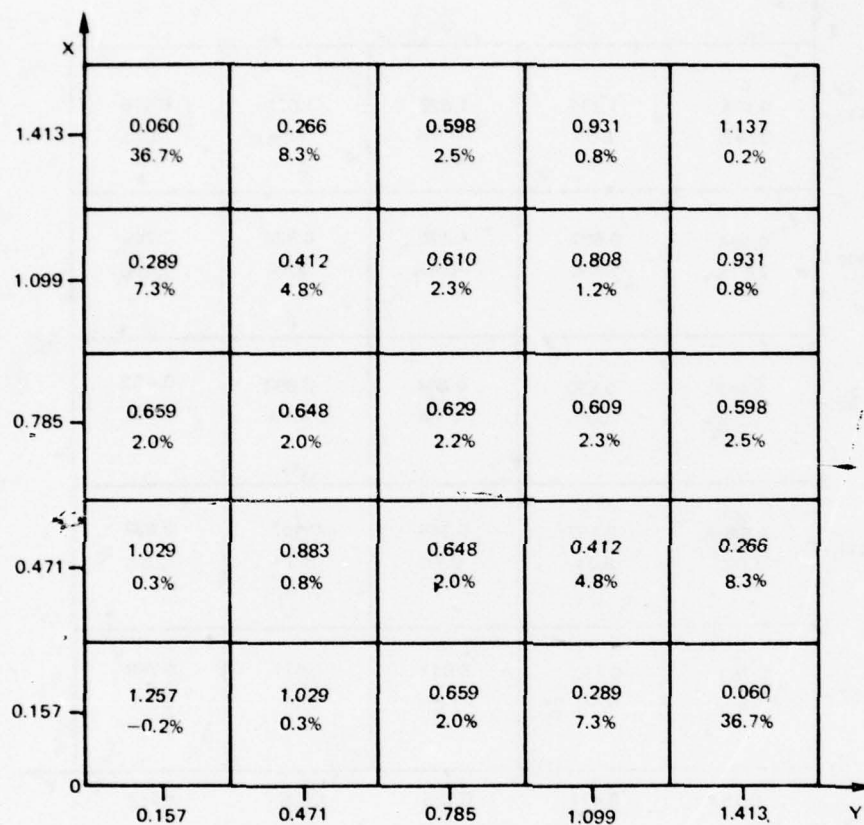


Figure 4Aa Comparison of Analytic and Computer Calculated Values of Perturbation Functions for Theta 11

THETA 22

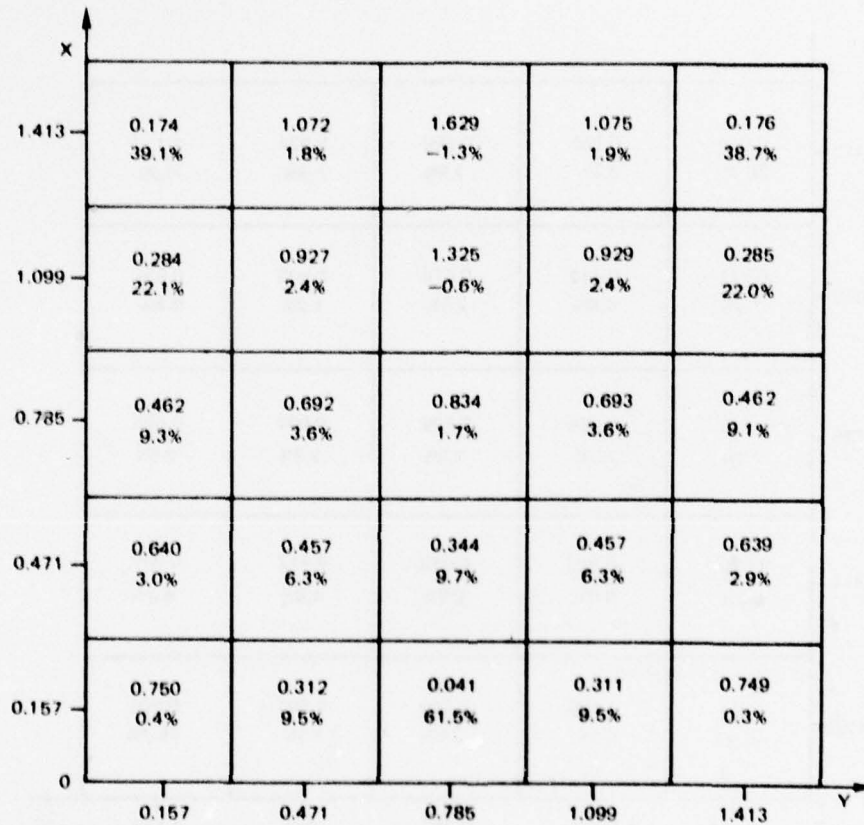


Figure 4Ab Comparison of Analytic and Computer Calculated Values of Perturbation Functions for Theta 22

THETA 12

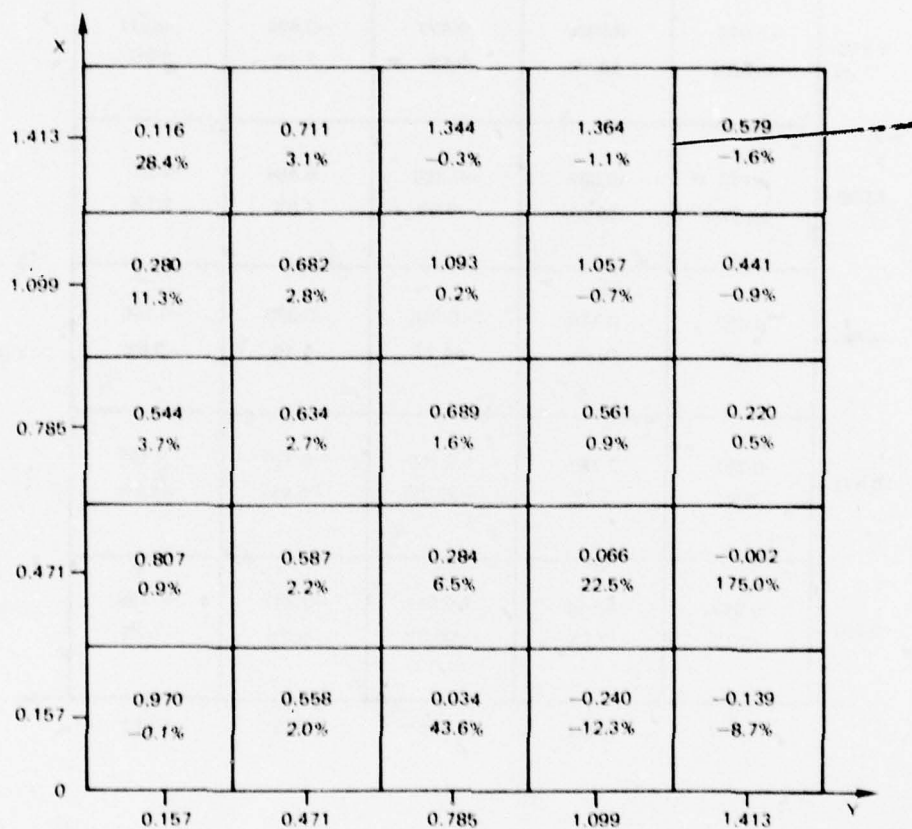


Figure 4Ac Comparison of Analytic and Computer Calculated Values of Perturbation Functions for Theta 12

THETA 21

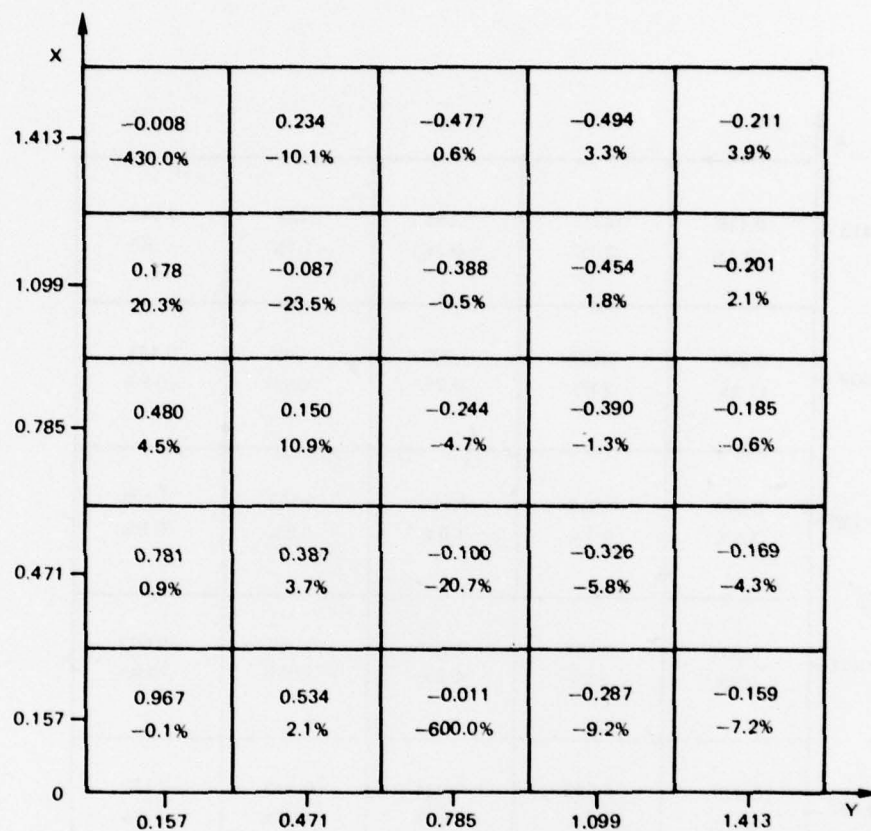


Figure 4Ad Comparison of Analytic and Computer Calculated Values of Perturbation Functions for Theta 21

Fringe data from the mode photographs was extracted by means of an x-y position digitizing table (279 mm square) made by Summagraphics, Inc., which was accurate to 0.005 inches (0.13 mm). This consisted of an active table, a position display, and a cursor, which itself consisted of cross hairs, position button, and flag buttons. The cross hairs were centered over a point on the table and the position button pushed. The X and Y values (in left-hand coordinates) for that point on the table, then appeared on the display, and were sent to the computer.

An overlay grid was drawn which had the same perimeter as the plate in the photographs and was divided into 36 sections (6 x 6), with the center of each section marked. This overlay grid, positioned and permanently fixed to the digitizer table, was used for all three modes to delineate the sections of evaluation. Each mode photograph was slid, in turn, under the grid for evaluation, insuring that the orientations, sizes, positions, and centers of each section would be the same for each mode.

For each section, the center point was recorded and the fringes were digitized, one at a time. An initial fringe number (the lowest) was entered into the computer, and after digitizing each fringe, the fringe number could be increased by one for the next fringe by pushing the cursor's flag button, or by entering it separately via the terminal. After each section was finished, an instruction (END) initiated computation of the mode coefficients for that section, and the process was repeated for the next section.

After the mode coefficients for all sections of all three modes were found, the A, B, and C coefficients for the first three modes were plotted on isometric paper. These drawings were examined for smoothness, and sections that appeared irregular were redigitized to check their accuracy. If new values were more regular, they were used instead.

The exact thickness of each section of the plate was measured (the thickness of the plate was roughly .3175 cm, but the programs allow for different thicknesses for each section), and the other constants determined experimentally ($E = 6.1 \times 10^{11}$ dynes/cm²), $\rho = 2.7$ (g/cm³), and $\nu = .31$). The mode coefficients, plate thickness, and other constants were used in the CHANGES program. Several different designs, with different mode perturbations were examined, and one such design was chosen for fabrication via the $(\Delta h/h)_m$ model. The design chosen had change parameters $\Delta_{11} = -.10$, $\Delta_{22} = +.10$, $\Delta_{21} = -.5994$, and $\Delta_{23} = .0880$. The first two correspond to changes in frequency of the first two modes of $\Delta\omega_1/\omega_1 = -.106$ and $\Delta\omega_2/\omega_2 = +.095$. The second two correspond to admixture coefficients of $C_{21} = -.2491$ and $C_{23} = -.0508$, which displace the node line of the second mode as shown in Fig. 5A. The ratios $\Delta h/h$ for each section are presented in Table IIIA, arranged in the 6 x 6 format of the sections on the plate. The RMS change in thickness was 0.284.

CLAMPED END

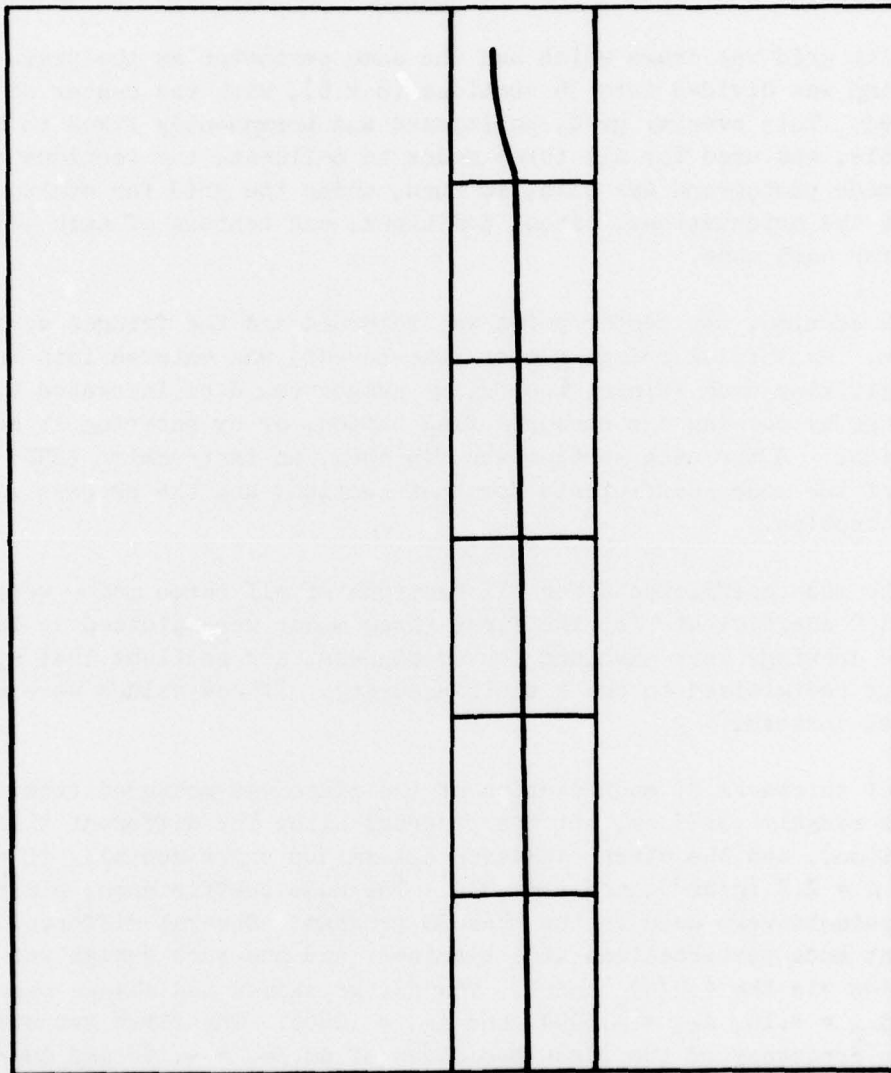


Figure 5A Plot of New Node Line Required for the Second Mode of a Modified Cantilever Plate

TABLE IIIA
FRACTIONAL THICKNESS CHANGES

Clamped End

-.109	-.169	-.356	-.294	-.084	+.196
+.011	+.028	-.007	-.017	+.003	+.016
-.058	+.111	+.193	+.222	+.147	+.047
-.230	+.006	+.135	+.294	+.265	+.218
-.506	-.107	+.135	+.284	+.404	+.281
-.847	-.352	+.153	+.468	+.506	+.504

Free End

Figure 6A shows the new plate, cemented and bolted to the same base block used for the uniform plate, and located in position with respect to the hologram recording apparatus. The frequencies of the first three modes for this plate were 106.3 Hz, 381.5 Hz, and 770.6 Hz, respectively, and a photograph of the holographic reconstruction of the new second mode is presented in Fig. 7A. The admixture coefficients were determined by digitizing section 34, the free end section that contained the displaced node line, and processing the data with the MODES program to get the bi-quadratic fit coefficients. These were then normalized and used with the normalized bi-quadratic fit coefficients for that section from the first three modes of the original uniform plate to form a set of simultaneous equations expressing the new mode shape as a linear combination of the old mode shapes. Solution of these equations gave the admixture coefficients $C_{21} = -0.217$ and $C_{23} = -0.0935$.

Given the plate with modified thickness, as tabulated in Table IIA, there are three ways to calculate the expected perturbations of the vibration modes. First, we may integrate $\Delta h/h$ times θ_{nk} as defined in Eq. (21A). Second, we may compute the corresponding variable $\Delta(h^3)/h^3 = ((1+\Delta h/h)^3 - 1)$ and integrate its product with $\theta_{nk}/3$. (The latter will correctly model changes in stiffness, whereas the former will correctly model changes in mass.) Third, we may use both parameters in Eq. (14A) to get the most accurate estimate of the first-order mode perturbations. The results of these three methods are tabulated in Table IVA, together with the experimentally determined values. Also tabulated are the root-mean-square differences between the experimental and each of the calculated values.

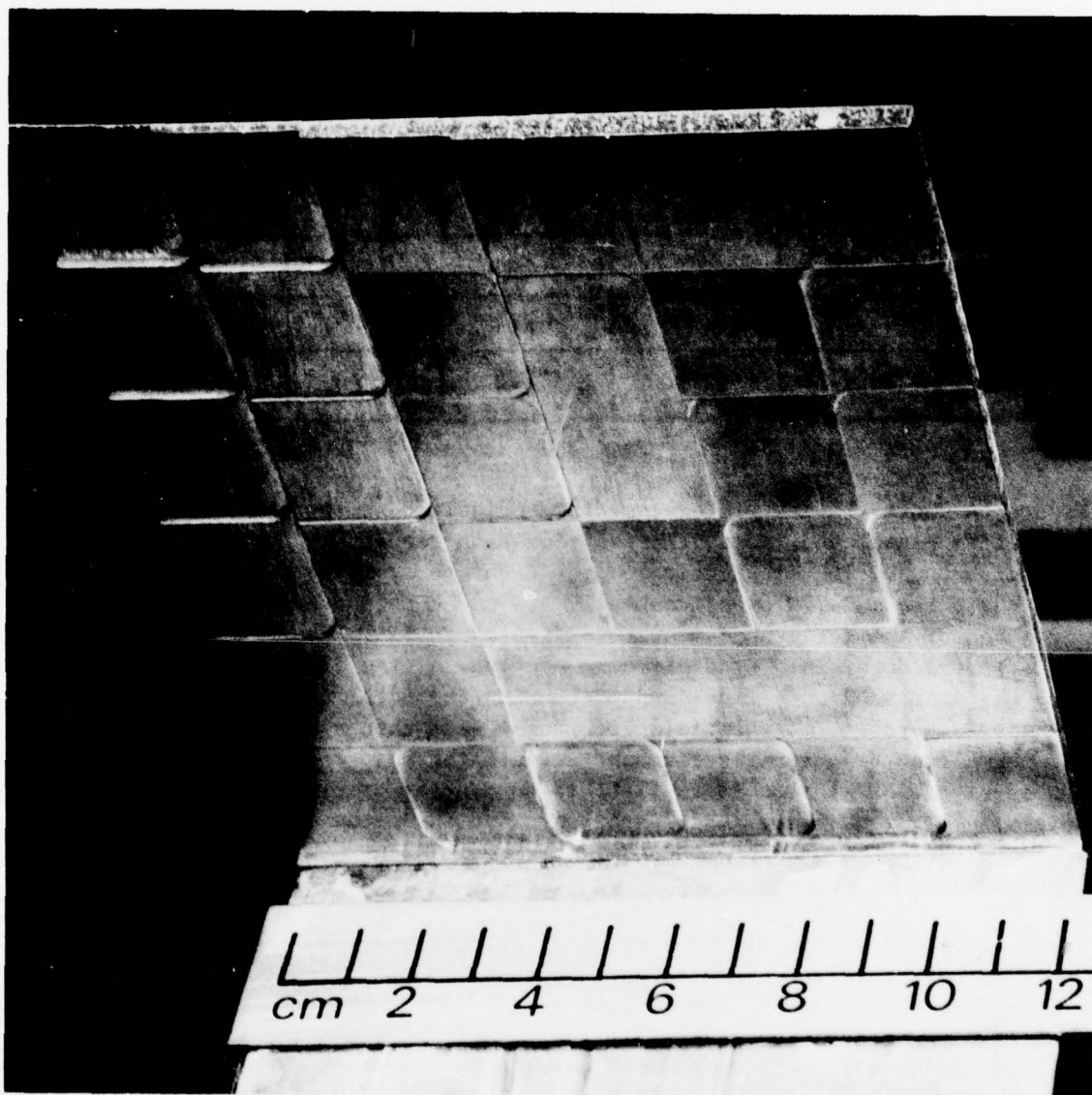


Figure 6A Photograph of a Cantilever Plate Modified to Have Variable Thickness so as to Meet Design Requirements



Figure 7A Photograph of a Hologram Reconstruction of a Cantilever Plate of Variable Thickness Vibrating in its Second Mode

TABLE IVA

PERTURBATION COMPARISONS

	Exper.	via $\Delta h/h$	via $\Delta(h^3)/h^3$	via Eq. (14)	(Des.-Exp.)
$\Delta\omega_1/\omega_1$	-.119	-.106	-.153	-.0593	+.013
$\Delta\omega_2/\omega_2$	+.143	+.095	+.0634	+.151	-.048
$\Delta\omega_3/\omega_3$	+.055	+.015	+.0246	+.0661	
C_{21}	-.217	-.2491	-.2443	-.2487	-.032
C_{23}	-.0935	-.0508	-.0553	-.0559	+.043
RMS diff.		0.0372	0.0471	0.0351	

(Note that the perturbation of the frequency of the third mode has been included, even though it was a parameter whose change was not specified. The perturbations calculated via $\Delta h/h$ (except for $\Delta\omega_3/\omega_3$) were the design objectives, and the RMS difference between these and the experimentally obtained results was .0365. This is 25 percent of the root-mean-square of the design changes. The last column presents the absolute difference between the original design requirements and the experimentally obtained values.)

Considering the complexity of the design requirements, and the size of the changes specified (admixture between modes 2 and 1 was 25 percent), we should regard the results as quite favorable. All constrained parameters did change in the correct direction, and it is reasonable to assume that a second iteration of the method, based on data taken from the second plate, would result in a plate whose vibratory performance would be quite close to specification. It should be noted that the largest change parameter, C_{21} , seems to have dominated the design at this step. The last column of Table IVA, which would provide the input requirements for the next iteration, shows a set of rather small changes well distributed between the four parameters.

In spite of the good agreement just discussed, considerable thought was given to the sources of error that might lead to the differences between the experimental and calculated perturbations. These could be: a) the stepwise nature of our plate, b) the scale of our changes being too large for first-order perturbation theory, and c) errors in our original calculations of second derivatives.

With respect to the stepwise structure of our plate, another plate, with slightly different design changes, was built both in steps and as a smoothly contoured surface interpolated between the centers of our sections. The experimentally determined perturbations showed less variation between these two designs than the variations in Table IIIA:

The scale of our changes, vis-a-vis the range of first-order perturbation theory, is the most likely source of error. Still, the errors inherent in the calculations of the second partial derivatives of the mode shapes needed to be examined. One way to do this is through orthogonality and Rayleigh-Quotient tests. To describe these, let us define a parameter, K_{nk} , as

$$K_{nk} = (\phi_k'')^T G (\phi_n'') dx dy. \quad (26A)$$

The orthogonality relationship derived in Ref. 4 requires that

$$K_{nk} = 0, \quad (27A)$$

and Rayleigh's principle requires that

$$K_{nn}/\omega_n^2 M_n = 1. \quad (28A)$$

K_{nn} should be the modal stiffness, K_n .

A program called CHECK was written to accept the data from the original uniform plate and compute the checks:

$$K_{nk}/(K_{nn}K_{kk})^{1/2}, \text{ when } n \neq k \text{ and}$$

$$K_{nn}/\omega_n^2 M_n, \text{ when } n=k.$$

The results are presented in Table VA.

TABLE VA

ORTHOGONALITY & RAYLEIGH QUOTIENT CHECKS

nk	check
12	-.014
13	-.126
23	+.0276
11	0.808
22	0.830
33	0.741

The first mode does not seem to have a stiffness function that is orthogonal with that of the third mode, and the three Rayleigh Quotients are all too small. It must be concluded, therefore, that there are significant errors in the second partial derivatives computed from the vibration mode data. This is understandable because these computations involved considerable modeling approximations to begin with. From a theoretical standpoint, these checks should be regarded as fundamental requirements for the modeling of the mode functions in the first place. Thus, what we really desire are values for the second partial derivatives, as close as possible to the ones experimentally calculated, that none-the-less satisfy orthogonality and Rayleigh-Quotient conditions. Fortunately, the minimization theory presented previously can be used to find these values, and this is presented in the next section.

Theory of Minimal Adjustments

We wish to make the smallest changes to the 2nd partial derivatives needed to pass the orthogonality and Rayleigh -Quotient conditions.

We represent the small changes by matrices, $(\Delta\phi_n'')$ to be added to the matrices (ϕ_n'') .

$$(\Delta\phi_n'') \equiv (\Delta\phi_n^{xx}, \Delta\phi_n^{yy}, \Delta\phi_n^{xy})^T$$

The orthogonality criteria and Rayleigh-Quotient criteria are defined by Eqs. (27A) and (28A), respectively. Since we have three modes we have only six constraints on the changes $(\Delta\phi_n'')$, as opposed to 36 sections for each of three modes. If we make the minimal changes to the 2nd derivatives, however, in the same way as the

minimal thickness changes were obtained, the problem becomes uniquely solvable to a first-order approximation. If we substitute $(\phi_n'' + \Delta\phi_n'')$ into Eqs. (27A) and (28A), the Rayleigh-Quotient and orthogonality conditions can be expressed to first-order as,

$$0 = \iint P_{nn} dx dy = \iint [(K_{nn} - \omega_n^2 M_n)/A_0 + (\Delta\phi_n'')^T G(\phi_n'') + (\phi_n'')^T G(\Delta\phi_n'')] dx dy \quad (29A)$$

when $n=k$, and

$$0 = \iint P_{nk} dx dy = \iint [K_{nk}/A_0 + (\Delta\phi_n'')^T G(\phi_k'') + (\phi_n'')^T G(\Delta\phi_k'')] dx dy, \quad (30A)$$

when $n \neq k$, and A_0 is the area of the plate. These criteria can be multiplied by an arbitrary constant and added to the equation expressing the mean-square change. In the case of two modes, we obtain the following equation for zero variance of the index of change,

$$0 = \delta \iint [(\Delta\phi_1'')^T I_1 (\Delta\phi_1'') + (\Delta\phi_2'')^T I_2 (\Delta\phi_2'') - \lambda_1 P_{11} - \lambda_2 P_{12} - \lambda_3 P_{22}] dx dy \quad (31A)$$

where I is the identity matrix.

The solution of this equation is found by setting the partials of the integrand, with respect to all components of $(\Delta\phi_1'')$ and $(\Delta\phi_2'')$, equal to zero. This gives

$$(\Delta\phi_1'') = G [(\phi_1''), (\phi_2''), 0] (\lambda), \text{ and} \quad (32A)$$

$$(\Delta\phi_2'') = G [0, (\phi_1''), (\phi_2'')] (\lambda). \quad (33A)$$

These equations for $(\Delta\phi_1'')$ and $(\Delta\phi_2'')$ can be substituted into Eqs. (29A) and (30A) to solve for (λ) . The three resulting equations may be put into matrix notation to be solved for (λ) , given which $\Delta\phi$ can be found via Eqs. (32A) and (33A).

$$\begin{pmatrix} -(K_{11} - \omega_1^2 M_1)/2 \\ -K_{12} \\ -(K_{22} - \omega_2^2 M_2)/2 \end{pmatrix} = \begin{bmatrix} \iint [(\phi_1''), (\phi_2''), 0]^T G G [(\phi_1''), (\phi_2''), 0] dx dy \\ + \iint [0, (\phi_1''), (\phi_2'')]^T G G [0, (\phi_1''), (\phi_2'')] dx dy \end{bmatrix} (\lambda) \quad (34A)$$

We wish to extend this process to adjust three modes. Equation (31A) then takes the form,

$$0 = \delta \iint [(\Delta\phi_1'')^T \underline{I} (\Delta\phi_1'') + (\Delta\phi_2'')^T \underline{I} (\Delta\phi_2'') + (\Delta\phi_3'')^T \underline{I} (\Delta\phi_3'') - \lambda_1 P_{11} - 2\lambda_2 P_{12} - 2\lambda_3 P_{13} - \lambda_4 P_{22} - 2\lambda_5 P_{23} - \lambda_6 P_{33}] dx dy . \quad (35A)$$

The solutions of the Euler equations in this case are

$$(\Delta\phi_1'') = \underline{G} [(\phi_1''), (\phi_2''), (\phi_3''), 0, 0, 0] (\lambda), \quad (36A)$$

$$(\Delta\phi_2'') = \underline{G} [0, (\phi_1''), 0, (\phi_2''), (\phi_3''), 0] (\lambda), \quad (37A)$$

$$(\Delta\phi_3'') = \underline{G} [0, 0, (\phi_1''), 0, (\phi_2''), (\phi_3'')] (\lambda) . \quad (38A)$$

For simplicity, let us call the matrices in the square brackets of Eqs. (36A)-(38A), \underline{Q} , \underline{R} , and \underline{S} , respectively. Then, the equations that must be solved for (λ) may be written in matrix form as

$$\begin{pmatrix} -(K_{11} - \omega_1^2 M_1)/2 \\ -K_{12} \\ -K_{13} \\ -(K_{22} - \omega_2^2 M_2)/2 \\ -K_{23} \end{pmatrix} = \left[\iint (\underline{Q}^T \underline{G} \underline{G} \underline{Q} + \underline{R}^T \underline{G} \underline{G} \underline{R} + \underline{S}^T \underline{G} \underline{G} \underline{S}) dx dy \right] (\lambda). \quad (39A)$$

As before, the solution for (λ) is used in Eqs. (36A)-(38A) to generate the changes in the second derivatives necessary to obtain values to satisfy the orthogonality and Rayleigh-Quotient conditions.

A program called MINFUDGE was written which performed the computations indicated above. Because the computation was actually a first-order approximation in Eqs. (29A) and (30A), two passes were required to obtain less than one percent error when the

adjusted second partial derivatives were put into the CHECK program. The result of both passes are presented in Table VIA.

TABLE VIA

CHECK PROGRAM RESULTS

nk	check(1)	check(2)
12	+.00514	+.000576
13	+.0169	+.00285
23	+.00368	+.00691
11	1.0306	1.00060
22	1.00931	1.00003
33	1.0250	1.00024

Finally, the adjusted values were used in the program that calculated the perturbations that should theoretically result from the design changes (Table IIIA). Only the computations via Eq. (14A) were made because these were presumed to be the most accurate. These are presented in Table VIIA.

TABLE VIIA

PERTURBATION CALCULATIONS

	MINFUDGE(1)	MINFUDGE(2)
$\Delta\omega_1/\omega_1$	-.0864	-.0822
$\Delta\omega_2/\omega_2$	+.175	+.174
$\Delta\omega_3/\omega_3$	+ +.099	+.096
C_{21}	-.2389	-.2400
C_{23}	+.0643	+.0637
RMS diff.	0.0327	0.0328

It can be seen from Table VIIA that application of the MINFUDGE program to the values for the second partial derivatives did reduce the RMS difference between the calculated and experimental perturbations. There seems to be little value in more than one application, however, and it cannot be said that the adjustment of the second derivatives made an outstanding improvement in the perturbation calculations. The rather large scale of the changes attempted in this design must be responsible, therefore, for the majority of the errors. It would be desirable to obtain a useful measure of the range of application of this technique. However, without a large number of comparisons between theory and experiment it is difficult to establish such a range. The RMS change in thickness, however, is probably the most relevant parameter, and the value of 28.4 percent for the case presented here is probably too large. Most probably, values between 10 percent and 15 percent would be more in keeping with the spirit of first-order perturbations.

Finally, some thought must be given to the extension of this method to more practical structures such as turbine blades, which would require knowledge of the vectorial mode displacements, and holographic determination of the in-plane strains as well as the bending strains. The technique of heterodyne hologram interferometry (Ref. 9) would have to be used to obtain these strain values. As yet, however, that type of holographic analysis has not been applied to vibration, but, in principle, could be by the addition of stroboscopic techniques. Dividing the structure into sections would still be the most practical realization of this procedure, although the computation of the perturbation functions would be more complex, of course. The simple products of mode functions would be replaced by scalar products of vectorial mode functions, and there would also be contributions due to the in-plane strain components. The complete description of what would be involved is well beyond the scope of this paper; however, it is our hope that our elementary results may stimulate further work in this area.

REFERENCES

1. Stetson, K. A. and P. A. Taylor: "The Use of Normal Mode Theory in Holographic Vibration Analysis with Application to an Asymmetrical Circular Disk." J. Phys E: Sci. Inst. 4, 1009, (1971).
2. Stetson, K. A. and P. A. Taylor: "Analysis of Static Deflections by Holographically Recorded Vibration Modes." J. Phys. E: Sci. Inst. 5, 923, (1972).
3. Bielawa, R. L.: "Techniques for Stability Analysis and Design Optimization with Dynamic Constraints of Nonconservative Linear Systems." AIAA Paper No. 71-388, AIAA/ASME 12th Structures Conference, Anaheim, California, 1971.
4. Stetson, K. A.: "Perturbation Method of Structural Design Relevant to Holographic Vibration Analysis." AIAA Journal 13, 457, (1975).
5. Stetson, K. A. and G. E. Palma: "Inversion of First-Order Perturbation Theory and Its Application to Structural Design.: AIAA Journal 14, 454, (1976).
6. Stetson, K. A. and I. R. Harrison: "Computer-Aided Holographic Vibration Analysis for Vectorial Displacements of Bladed Disks." Applied Optics (in printing).
7. Schultz, D. G. and J. L. Melsa: State Functions and Linear Control Systems. McGraw-Hill, New York, Chap. 6, pp. 197-210, 1967.
8. Hoffman, K. and R. Kunze: Linear Algebra. Prentice-Hall, Englewood, N. J., Chap. 8, pp. 224-225, 1961.
9. Dändliker, R., E. Marom, and F. M. Mottier: "Two-Reference-Beam Holographic Interferometry." J. Opt. Soc. Am., 66, 23, (1976.)